Regulatory Toxicology and Pharmacology 159 (2025) 105794

Contents lists available at ScienceDirect

Regulatory Toxicology and Pharmacology

journal homepage: www.elsevier.com/locate/yrtph

Next generation risk assessment of hair dye HC yellow no. 13: Ensuring protection from liver steatogenic effects

Sara Sepehri, Dinja De Win, Anja Heymans, Freddy Van Goethem, Robim M. Rodrigues, Vera Rogiers, Tamara Vanhaecke *

Department of In Vitro Toxicology and Dermato-Cosmetology (IVTD), Vrije Universiteit Brussel, Brussels, Belgium

ARTICLE INFO

Handling Editor: Dr. Martin Van den berg

Keywords:
Next generation risk assessment
New approach methodologies
Cosmetics
Human stem cells
Liver steatosis

ABSTRACT

This study employs animal-free Next Generation Risk Assessment (NGRA) principles to evaluate the safety of repeated dermal exposure to 2.5% (w/w) HC Yellow No. 13 (HCY13) hair dye. As multiple *in silico* tools consistently flagged hepatotoxic potential, likely due to HCY13's trifluoromethyl group, which is known to interfere with hepatic lipid metabolism, liver steatosis was chosen as the primary mode of action for evaluation. AOP-guided *in vitro* tests were conducted, exposing human stem cell-derived hepatic cells to varying HCY13 concentrations over 72 h. The expression of 11 lipid metabolism-related marker genes (*AHR*, *PPARA*, *LXRA*, *APOB*, *ACOX1*, *CPT1A*, *FASN*, *SCD1*, *DGAT2*, *CD36*, and *PPARG*) and triglyceride accumulation, a phenotypic hallmark of steatosis, were measured. PROAST software was used to calculate *in vitro* Points of Departure (PoD_{NAM}) for each biomarker. Using GastroPlus 9.9, physiologically-based pharmacokinetic (PBPK) models estimated internal liver concentrations ($C_{max\ liver}$) of HCY13, ranging from 4 to 20 pM. All PoD_{NAM} values significantly exceeded the predicted $C_{max\ liver}$, indicating that HCY13 at 2.5% (w/w) is unlikely to induce liver steatosis under the assumed conditions. This research demonstrates the utility of NGRA, integrating AOP-based *in vitro* assays and computational models to protect human health and support regulatory decision-making without animal testing.

1. Introduction

Driven by scientific advancements, ethical concerns, economic considerations, and legislative changes, modern toxicology increasingly prioritizes using animal-free methods for chemical safety assessment. New Approach Methodologies (NAMs) are central to this paradigm shift by incorporating innovative techniques such as *in vitro* methods (e.g. human cell cultures), *in silico* approaches (computer modeling), *in chemico* techniques (chemical interactions), and *ex vivo* (isolated tissues) methods. These methodologies offer the potential to provide more human-relevant data, reducing reliance on animal testing and improving the efficiency and accuracy of risk assessments through a mechanistic approach. The Next Generation Risk Assessment (NGRA) exemplifies the integration of NAMs within a tiered framework tailored to a specific exposure scenario. This approach is hypothesis-driven and focused on harm prevention in humans. It involves evaluating existing data and generating new targeted information using NAMs in a tiered, iterative manner to ensure a comprehensive chemical safety assessment. Supported by recent research and guidelines, NGRA emphasizes transparent documentation of the logical framework and uncertainties (Dent et al., 2018; Dent et al., 2021; Gautier et al., 2020; Ouedraogo et al., 2022; Najjar et al., 2024; Assaf Vandecasteele et al., 2021; Bury et al., 2021a; Directorate and Committee, 2021; Gilmour et al., 2023; Luo et al., 2023; OECD, 2023; Ebmeyer et al., 2024; Baltazar et al., 2020).

Being exposure-led, NGRA emphasizes that a chemical is unlikely to cause adverse effects on human health if internal exposure levels are well below those needed for biological activity. Physiologically-based pharmacokinetic (PBPK) models are used to estimate internal exposure. In contrast, *in silico* models and human-relevant *in vitro* assays are employed to flag and assess potential effects by targeting early biological changes before adverse effects manifest, translating into a Point of Departure (PoD_{NAM}). A thorough understanding of the biological pathways underlying adverse outcomes significantly increases confidence that the assessment is protective for the mode of action (MoA). Adverse

* Corresponding author.
E-mail addresses: sara.sepehri@vub.be (S. Sepehri), dinja.de.win@vub.be (D. De Win), anja.heymans@vub.be (A. Heymans), freddy.van.goethem@vub.be (F. Van Goethem), robim.marcelino.rodrigues@vub.be (R.M. Rodrigues), vera.rogiers@vub.be (V. Rogiers), tamara.vanhaecke@vub.be (T. Vanhaecke).

https://doi.org/10.1016/j.yrtph.2025.105794
Received 9 October 2024; Received in revised form 17 February 2025; Accepted 27 February 2025
Available online 28 February 2025
0273-2300/© 2025 The Authors. Published by Elsevier Inc. This is an open access article under the CC BY-NC-ND license (http://creativecommons.org/licenses/by-nc-nd/4.0/).

Outcome Pathways (AOPs) provide a framework by linking mechanistic molecular and cellular events to adverse outcomes. They establish connections between Key Events (KEs) through Key Event Relationships (KERs), starting with the Molecular Initiating Event (MIE) and culminating in the Adverse Outcome (AO) at the organism level. This systematic approach enables a more detailed and mechanistic understanding of how chemicals cause harm, thereby enhancing the predictive power and reliability of NGRA (Bajard et al., 2023; Pallocca et al., 2022). Dividing the PoD_{NAM} by the estimated internal exposure yields the Bioactivity-Exposure Ratio (BER). A BER greater than 1 generally suggests that the bioactivity threshold surpasses estimated human exposure, indicating potential safety (Health Canada, 2021; Middleton et al., 2022). However, the interpretation of BER values is still being refined, and further evidence is needed to establish firm regulatory thresholds for different types of NAM data (Wambaugh, 2024; Cronin et al., 2023).

Since March 2013, when the European Union (EU) fully implemented the ban on animal testing and marketing for cosmetics, the importance of NGRA has grown. This shift became even more crucial because determining a PoD from repeated dose toxicity studies, as traditionally done in animals, was no longer possible. NGRA case studies have proven effective in protecting human health, particularly for local toxicity endpoints such as skin sensitization (Gilmour et al., 2023; OECD, 2023; Bialas et al., 2023). However, introducing new cosmetics on the EU market remains challenging due to the need for animal-free methods to assess complex toxicological endpoints like repeated dose systemic and organ toxicity. Although some NGRA case studies assessing systemic toxicity have been conducted using data-rich, generally safe compounds like fragrances and preservatives (Directorate and Committee, 2021; Ebmeyer et al., 2024; Baltazar et al., 2020; Troutman et al., 2015; OECD, 2020; Bury et al., 2021b), a critical challenge remains: determining whether NGRA can also effectively identify and prohibit toxic compounds from the market. Achieving a higher confidence level requires evaluating a broader range of ingredients. In this context, this case study applies NGRA principles using an *ab initio* approach, assuming no existing *in vivo* safety data, to assess the hypothetical risk of triggering liver steatosis from HC Yellow No. 13 (HCY13) (Fluorgelb II), a widely used fluorinated hair dye. Although both hepatotoxicity and mutagenicity were flagged during *in silico* hazard identification, liver steatosis was selected as the primary MoA for evaluation.

Regulated under Annex III of the Cosmetic Regulation (EC) No. 1223/2009, HCY13 is currently permitted at a maximum on-head concentration of 2.5% (w/w) in both oxidative and non-oxidative hair dye formulations ().

2. Materials and methods

Fig. 1 illustrates an adapted NGRA framework for the *ab initio* scenario, where safety evaluation is carried out based on hypothesis-driven *in vitro* testing combined with computational modeling and a BER for risk characterization. Berggren et al. (2017) suggest exit points in the lower tiers (0 and 1) via Threshold of Toxicological Concern (TTC) or Read-Across (RAx) approaches. However, RAx was deemed unsuitable in this study due to the lack of data-rich structural analogs for HCY13. Instead, the internal TTC (iTTC) approach has been applied to assess potential risks from identified metabolites (Hewitt et al., 2013; Pawar et al., 2019; Lester et al., 2023; Lizarraga et al., 2023; Berggren et al., 2017). The overall workflow includes three tiers and 10 steps, with relevant *in silico* tools and the used *in vitro* model briefly outlined in Fig. 1. Supporting data for interactions with transporters, Cytochromes P450, and UGT (Uridine 5′-diphosphate-glucuronosyltransferases) enzymes (Tier 0) are detailed in Supplementary Material 1, which also includes information on the predicted metabolites. Information on analogs used in Tier 1 during the Hypothesis Generation, following step 5 of the Weight-of-Evidence (WoE) approach, is in Supplementary Material 2. For Tier 2: Bioactivity Characterization, Supplementary Material 3 provides cell culture details, Supplementary Material 4 covers the Neutral Red Uptake (NRU) assay for cell viability, and Supplementary Material 5 includes the functional and gene expression assays related to lipid accumulation. The Benchmark Concentration (BMC) approach is described in Supplementary Material 6.

3. Results

Tier 0: Identifying the Exposure Scenario, Chemical identity, and Collecting Data.

3.1. Identify use/exposure scenario: calculation of the externally applied dose

Table 1 presents external dose calculations assuming the maximum permitted concentration of HCY13 for a conservative analysis (SCCS/1322/10, 2011). While commercial products may not always use the highest concentration, proprietary formulations are generally inaccessible, justifying the use of the regulatory maximum. All calculations assume 100% purity of HCY13.

To adopt a conservative approach, as outlined in SCCS/1647/22 (SCCS/1647/22, 2023), a daily exposure value in mg/day is not calculated for hair dyes due to their low frequency of application, i.e. once per week for non-oxidative hair dyes. Consequently, the daily dose is not averaged over a 7-day period in this context.

3.2. Chemical identity: molecular structure

Characterizing the physical form, molecular weight, and physicochemical specifications of HCY13 is essential for understanding its behavior (SCCS/1647/22, 2023). The chemical identity specifications of HCY13 retrieved from SCCS/1322/10 (2011) are summarized in Table 2 (SCCS/1322/10, 2011). HCY13, a yellow powder, contains a nitro group (NO_2, circled in green) and a trifluoromethyl group (CF_3, circled in orange), significantly influencing its reactivity and cosmetic use. The NO_2 group contributes to HCY13's vibrant color properties, making it a valuable dye in cosmetic formulations. However, NO_2 groups are electron-withdrawing, affecting the electronic distribution within the molecule and, hence, its reactivity and stability (Kumar et al., 2021). They can undergo metabolic activation in biological systems, forming reactive intermediates, potentially leading to cytotoxicity or mutagenicity, raising concerns about the safety of prolonged exposure to NO_2-containing dyes (SCCS Opinion on Nitrosamines and, 2012). Additionally, the presence of a CF_3 group in HCY13 categorizes it as a non-polymeric per- and polyfluoroalkyl substance (PFAS), according to OECD: "any chemical with at least a perfluorinated methyl group (CF_3) or a perfluorinated methylene group (CF_2) is a PFAS (without any H/Cl/Br/I atom attached to it)" (Wang et al., 2021; Hammel et al., 2022). Exposure to PFAS has been linked to numerous adverse health effects, notably liver steatosis or fatty liver disease. This association is linked to PFAS compounds' capacity to disrupt lipid metabolism, triggering oxidative stress and impairing fatty acid (FA) β-oxidation, resulting in lipid accumulation within hepatocytes. While the precise mechanism remains elusive, research suggests the potential involvement of PPARA activation and perturbations in the lipolysis-lipogenesis balance and the depletion of liver glutathione levels, as evidenced across various epidemiological, animal, and *in vitro* studies (Zhao et al., 2023; David et al., 2023; Zhang et al., 2023; Sadrabadi et al., 2024; Chen et al., 2020; Khan et al., 2023; Hyötyläinen et al., 2021; Lu et al., 2019; Goodrich et al., 2023; India-Aldana et al., 2023; Ojo et al., 2021). The CF_3-group in HCY13 may thus contribute to such effects.

While both hepatotoxicity and mutagenicity were predicted, only liver steatosis was selected to exemplify NGRA for this MoA. Indeed, the CF_3 group in HCY13 might play a critical role in reducing its mutagenic potential. As a strong electron-withdrawing group, -CF_3 lowers the electron density on the aromatic ring and introduces steric hindrance,

TIER 0

Gathering Information

1. Identify Use/Exposure Scenario:
HCY13 is used as a 2.5% (w/w) (max. allowance) dye in non-oxidative hair color, dissolved in hot water.

2. Chemical Identity:
HCY13 identity data (structural formula, CAS number, INCI name, molecular weight) obtained from SCCS/10/1322 (2011), SMILES notation used for modeling.

3. Collect Supporting Data:
Physico-Chemical Properties: Sourced via SCCS/1322/10 (2011).
***In Silico* ADME Prediction:** Use SMILES with ADMET Predictor 11.0 and OECD QSAR Toolbox for *in silico* simulations of key absorption, distribution, metabolism and excretion parameters. (Supplementary Material 1)
Active Group Predictions: Using HCY13's structure and SMILES annotation, four *in silico* tools were applied to identify hepatotoxicity alerts: OECD QSAR Toolbox, VEGA QSAR, SA Predictor, and Vienna Livertox Workspace.

TIER 1

Hypothesis Generation

4. Obtaining Internal Liver Concentration:
Dermal Route PBPK Modeling: Using 0.13% of the applied dose for the dermal bioavailability (SCCS/1647/22(2023)). Two kinetic models (compartmental and PBPK) are used with parameters imported into Gastroplus 9.9 via ADMET Predictor 11.0. The compartmental model adjusts BW and liver metabolism, while the PBPK model, tailored for a 30-year-old female (75 kg), adjusts renal clearance and liver metabolism. A consistent BW of 75 kg is used for all exposure assessments.

5. Mode of Action (MoA) Hypothesis Generation:
Weight-of-Evidence (WoE) Analysis: Using WoE analysis, formulate a steatogenic liver toxicity hypothesis based on molecular structure and active group predictions. Using GenRA, identify structural analogs with a Tanimoto coefficient >0.8 and evaluate structural alerts with HESS via the OECD QSAR Toolbox. (Supplementary Material 2)

TIER 2

Bioactivity Characterization

6. Targeted Testing Using Human-Relevant Test System *In Vitro*:
AOP-Based Liver Steatosis Characterization: hSKP-HPC used to assess HCY13 impact on lipid metabolism following the AOP suggested by Verhoeven *et al.* 2024.
hSKP-HPC Cell Culture: hSKP cells isolated and differentiated into hepatocyte-like cells. (Supplementary Material 3)
Exposure Setup: Post cytotoxicity assessment, cells exposed to sub-cytotoxic concentrations of HCY13 (10-100 μM) for 72h, Na-VPA (1.2-12 mM) as positive and solvent-only negative controls. (Supplementary Material 4)
Assays: (Supplementary Material 5)
Lipid Accumulation Assessment: *Neutral Lipid Staining* according to Boeckmans *et al.* (2021). *Flow Cytometric Analysis of Neutral Lipids* according to Boeckmans *et al.* (2020). *TG Quantification* using the E-BC-K261 kit from Elabscience according to the manufacturer protocol.
Gene Expression (RT-qPCR): Key genes related to lipid metabolism and liver function analyzed: AHR, PPARA, LXRA, APOB, ACOX1, CPT1A, FASN, SCD1, DGAT2, CD36, and PPARG.

7. Biokinetic Refinement (Population Estimation, Metabolites Refinement):
PBPK Models and Population Simulation: Gastroplus 9.9's population simulator with Monte Carlo simulations (PEAR) was used to estimate liver concentrations ($C_{max\ liver}$) and variability across a diverse virtual population.
Metabolites Refinement: The iTTC approach, as outlined by Dent *et al.* (2021), was applied to assess potential liver risks from predicted metabolites. Using GastroPlus 9.9, maximum plasma concentrations were predicted for both single-object and population levels.

8. Points of Departure Calculation Using BMC Approach:
BMC Analysis: Concentration-response curves for triglyceride accumulation were modeled with a BMR of 20%, while gene expression changes were analyzed with a BMR of 50%. These BMR values were used in PROAST 70.1 (https://proastweb.rivm.nl) software to generate BMC_L confidence intervals, with the BMC_L serving as the PoD_{NAM} for each biomarker. (Supplementary Material 6)

TIER 3

Risk Characterization

9.Calculation of Bioactivity-Exposure Ratio Based on Lowest PoD_{NAM}:
BER Calculation: The BER was calculated by comparing the lowest *in vitro* bioactivity threshold (PoD_{NAM}), derived from the lowest BMC_L, with predicted human liver exposure levels ($C_{max\ liver}$). A BER greater than 1 indicates a potentially sufficient margin of safety. In contrast, a BER below 1 may warrant further investigation or raise potential concerns, depending on the context and uncertainty factors.

10.Risk Evaluation and Uncertainties Assessment:
Uncertainty Classification: Based on the robustness and reliability of the data, certainties were qualitatively classified as low (L), medium (M), or high (H).

(caption on next page)

Fig. 1. The NGRA framework used to assess the safety of 2.5% (w/w) HC Yellow No. 13 under non-oxidative conditions, focusing on liver steatosis. The workflow is divided into 4 tiers, covering 10 steps: **Tier 0: Gathering Information** (Steps 1–3): Includes identifying the use/exposure scenario, chemical identity, and supporting data, including *in silico* ADMET predictions and physicochemical properties. **Tier 1: Hypothesis Generation** (Steps 4–5): Involves estimating internal liver concentrations through PBPK modeling (dermal exposure) and generating a MoA hypothesis based on WoE analysis. **Tier 2: Bioactivity Characterization** (Steps 6–7): Involves targeted *in vitro* testing using hSKP-HPC for liver steatosis endpoints and refining biokinetic and population-level estimates. **Tier 3: Risk Characterization** (Steps 8–10): Includes determining PoD using BMC analysis, calculating the BER, and evaluating uncertainties for risk assessment. [HCY13: HC Yellow No. 13, CAS: Chemical Abstracts Service, INCI: International Nomenclature of Cosmetic Ingredients, SCCS: Scientific Committee on Consumer Safety, SMILES: Simplified Molecular Input Line Entry System, OECD QSAR Toolbox: Organisation for Economic Co-operation and Development Quantitative Structure-Activity Relationship Toolbox, PBPK: Physioligically-based Pharmacokinetic, BW: Body Weight, MoA: Mode of Action, WoE: Weight-of-Evidence, GenRA: Generalized Read-Across, HESS: Hazard Evaluation Support System, hSKP-HPC: human Skin-derived Precursor Hepatocyte-like Cells, AHR: Aryl Hydrocarbon Receptor, PPARA: Peroxisome Proliferator-Activated Receptor Alpha, LXRA: Liver X Receptor Alpha, APOB: Apolipoprotein B, ACOX1: Acyl-CoA Oxidase 1, CPT1A: Carnitine Palmitoyltransferase 1A, FASN: Fatty Acid Synthase, SCD1: Stearoyl-CoA Desaturase 1, DGAT2: Diacylglycerol O-Acyltransferase 2, CD36: Cluster of Differentiation 36, PPARG: Peroxisome Proliferator-Activated Receptor Gamma, TG: Triglyceride, NaVPA: Sodium Valproate, PEAR: Population Estimates for Age-Related Physiology, iTTC: internal Threshold of Toxicological Concern, BMC: Benchmark Concentration, PoD: Point of Departure, NAM: New Approach Methodologies, BMR: Benchmark Response, BMC_L: Benchmark Concentration Lower Bound, BER: Bioactivity Exposure Ratio].

Table 1
Calculation of the externally applied dose using 2.5% (w/w) HCY13 in a hypothetical hair dye formulation (SCCS/1647/22, 2023). *$Assuming that* 1 ml *of product is equivalent to 1 g [C: Concentration, A: Amount per application, R: Retention factor].*

Use concentration (C)	2.5% (maximum permitted)	Annex III of EU legislation, Ref no. 261
Amount per application (A)$	**35 g**	SCCS/1647/22 (SCCS/1647/22, 2023)
Retention factor (R)	**0.1**	SCCS/1647/22 (SCCS/1647/22, 2023)
- > Amount applied (C/100*A*R) = (2.5/100)*35*0.1*1000 = **87.5 mg**		

Table 2
Chemical identity specifications and physicochemical properties. Rows "Name" to "Relative density", of HCY13 retrieved from (SCCS/1322/10, 2011). Rows *"ECCS classification" to "Interactions with transporters and Cytochromes P450s" predicted by ADMET Predictor 11.0.* Supplementary Material 1 *presents the predicted interactions of HCY13 with various transporters and cytochrome P450 enzymes, as determined by ADMET Predictor 11.0, along with specific kinetic parameters where applicable. [ECSS: Extended Clearance Classification System].*

Name	HC Yellow 13
CAS no.	10442-83-8
Molecular formula	$C_9H_9F_3N_2O_3$
2D chemical structure	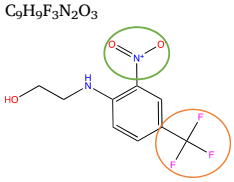
INCI names	N-(2-Hydroxyethyl)-2-nitro-4-trifluormethyl-aniline; 1-(2-Hydroxyethyl)amino-2-nitro-4-trifluormethylbenzene
Commercial names	Fluorgelb II, Cos 128, COLIPA B102
Molecular weight	250.18 g/mol
Log $P_{o/w}$ at pH 7, 23°C	2.54 (determined by EC-A.8 method)
Appearance	Yellow crystalline powder
Purity	99% HPLC
Water solubility at 20°C	506 mg/L (determined by EC-A.6 method)
Melting point	74.7 °C
Boiling point	227.1 °C
Vapor pressure at 20°C	3.1*10^-8 hPa
Relative density at 20°C	1.45
ECCS classification	2
Fraction unbound in plasma (Fup)	8.819 %
Volume of distribution human (V_d)	1.571 L
Blood:plasma ratio (Rbp)	1.003
Hepatic intrinsic clearance (CL)	30.31 μL/min/million hepatocytes
Renal excretion	No
Interaction with transporters and Cytochromes P450s	Supplementary Material 1

hampering metabolic activation pathways such as hydroxylamine formation, typically associated with DNA reactivity (Hewitt et al., 2013; Pawar et al., 2019; Lester et al., 2023; Lizarraga et al., 2023).

3.3. Collect supporting data

The basic physicochemical properties of HCY13 are shown in Table 2 (). To ensure chemical structure identification is interpretable by *in silico* software, formats like the Simplified Molecular Input Line Entry System (SMILES) have been used (Weininger, 1988).

3.3.1. In silico absorption, distribution, metabolization, excretion (ADME) prediction

A key benefit of employing ADMET Predictor 11.0 software, developed by Simulation plus®, is its capability to directly import ADME parameters into subsequent software (GastroPlus) to predict the maximum liver concentration. Both software tools were utilized under the Simulation Plus University + program, providing free academic access. To accurately estimate the internal exposure concentration using PBPK modeling in Tier 1, extra chemical-specific parameters such as Blood: plasma ratio (Rbp), the fraction unbound in plasma (Fup), liver clearance (CL), and the volume of distribution (V_d), are needed as input data. In this study, the predicted required data are summarized in Table 2. HCY13, classified as class 2 under the Extended Clearance Classification System (ECCS), is primarily cleared via liver metabolism (Varma et al., 2015). It exhibits a Fup of 8.819%, indicating high plasma protein binding, which suggests that the majority of the compound is bound to plasma proteins such as albumin, thereby reducing the free fraction availabile for tissue distribution and metabolism (Yun et al., 2021). With a V_d of 1.571 L, HCY13 remains largely confined to the vascular space and does not extensively distribute into tissues. The Rbp near 1 suggests that HCY13 has similar affinities for plasma and the cellular components of the blood. Collectively, these characteristics suggest that HCY13 exhibits extensive plasma protein binding and is primarily confined to the vascular compartment with limited tissue interaction. HCY13 shows a high affinity for uptake via organic anion transporter 1 (OAT1, Km = 22.502 μM) but low affinity for organic cation transporter 1 (OCT1, K_m = 193.009 μM), suggesting differential cellular uptake influenced by transporter expression (Nigam et al., 2015; Roth et al., 2012; Suo et al., 2023; Lozano et al., 2013; Granados et al., 2021). Furthermore, HCY13 is unlikely to inhibit the Bile Salt Export Pump (BSEP), as indicated by a high IC_{50}(log) of 73.4 μM, suggesting a minimal impact on bile acid transport (Chan and Benet, 2018). HCY13 exhibits rapid hepatic metabolism with an intrinsic clearance of 30.31 μL/min/million hepatocytes, as detailed in Supplementary Material 1. It is likely metabolized by Cytochrome P450 (CYP) enzymes (particularly CYP3A4, CYP1A2, CYP2C8, CYP2C19, and CYP1A2) and Uridine 5′-diphosphate-glucuronosyltransferases (UGT) enzymes (UGT1A8, UGT1A9, UGT2B7) (Rowland et al., 2013). It strongly inhibits CYP1A2 (K_i (inhibition constant) = 3.276 μM, prediction confidence: 95%),

suggesting potential for drug-drug interactions affecting CYP1A2 substrates (Bhatt et al., 2022). Regarding the identified metabolites, simulations revealed potential metabolites in various environments, including rat liver, human skin, gut microbiome, and liver. In skin metabolism, the OECD QSAR Toolbox identified a single metabolite, M3 (OCCN=C1C=CC(=CC1 = [N+](O)[O-])C(F)(F)F), the imino-enamino tautomer of the parent compound. In contrast, the human microbial and rat liver simulations produced 16 and 4 metabolites, respectively, with one common metabolite, M1 (NC1=CC=C(C(F)(F)F)C=C1[N+]([O-]) = O). Further analysis with ADMET Predictor also identified M1 and another metabolite, M2 (O=CCNC1=CC=C(C(F)(F)F)C=C1[N+]([O-]) = O), in the human liver. These metabolites are primarily processed by CYP1A2, CYP2C19, and CYP3A4, with M1 metabolized at 74% and M2 at 26%, specifically M1 by CYP1A2 (10.7%), CYP2C19 (49.1%), and CYP3A4 (4.2%), and M2 by CYP2C19 (21.8%) and CYP3A4 (0.9%) (Supplementary Material 1).

3.3.2. Active group prediction

Centering on the molecular structure of HCY13, which includes the nitro and the trifluoromethyl hepatotoxic groups, and considering ADME predictions indicating liver excretion as the primary route, our analysis further focused on its possible hepatotoxic potential. Using SMILES annotation, four freely available *in silico* tools were applied:

- HESS (OECD QSAR Toolbox): A mechanistic tool utilizing the Hazard Evaluation Support System (HESS), which categorizes *in vivo* toxicity for 500 chemicals across 14 types (Sakuratani et al., 2013; Safety Assessment Division, Chemical Management Center, National Institute of Technology and Evaluation, 2023), identified a flutamide-induced hepatotoxicity alert with a 61% similarity index using the Dice method.
- VEGA-IRFM: A mechanistic tool employing the IRFMN-v.1.0.1 hepatotoxicity model with SARpy, which identifies structural alerts, highlighted the CF_3-group as a relevant hepatotoxic fragment with 86% accuracy (Pizzo et al., 2016; Gadaleta and Benfenati, 2022).
- SA Predictor: This statistical tool, which offers rapid toxicity screening through structural alerts (61), flagged both NO_2 and CF_3 groups as potential hepatotoxic moieties.
- Vienna Livertox Workspace: A mechanistic tool using Drug-Induced Liver Injury (DILI) models with a random forest algorithm (500 trees and RDKit descriptors) based on a dataset of 966 compounds predicted a 0.72 positive DILI effect in humans with accuracies ranging from 0.59 to 0.68 (Montanari et al., 2020; Vienna LiverTox, 2020).

HCY13 falls within the applicability domain of all four models. The combined use of statistical and mechanistic *in silico* tools, as recommended by the International Cooperation on Cosmetics Regulation (ICCR) (Teixeira do Amaral et al., 2014), consistently indicated a hepatotoxic alert for HCY13.

Tier 1: Obtaining Internal Organ Concentrations and Hypothesis Generation.

3.4. Obtaining the internal liver concentration using PBPK modeling via dermal route administration

To determine the internal liver concentration, it is essential to first calculate the fraction of the applied hair dye dose that penetrates the scalp and thus an estimate of HCY13's dermal absorption is needed. This study used a dermal absorption value of 3.13 μg/cm^2 (mean + 2 SD), corresponding to 0.13 % of the applied dose. This value was derived from an *in vitro* dermal absorption study (compliant with OECD 428) conducted on pig skin with a typical non-oxidative hair dye formulation containing 2.5% (w/w) HCY13, as detailed in SCCS/1322/10 (SCCS/1322/10, 2011). For an externally applied dose of 87.5 mg, this results in a dermally bioavailable dose of 0.11 mg.

3.4.1. PBPK modeling

Following predictions from the ADMET Predictor, GastroPlus 9.9 was used to estimate maximum liver concentrations ($C_{max\ liver}$) using two deterministic kinetic models: a compartmental model and a PBPK model. The software was accessed through the Simulation Plus University + program at no cost. The compartmental model characterizes compound distribution and elimination using parameters such as CL, V_d, and transfer rate constants (Chen and Om Abuassba, 2021) and allows adjustments for BW and liver clearance parameters by selecting the hepatic clearance mechanism (cytochromes, total microsomes, and hepatocytes). All options were explored due to the lack of precise data on HCY13's metabolism.

The PBPK model, tailored for a 30-year-old female weighing 75 kg, provides a detailed representation incorporating tissue weights, volumes, and physiological parameters, allowing adjustments for renal clearance and liver metabolism (Jones and Rowland-Yeo, 2013; Simulations-plus, 2017). A consistent Body Weight (BW) of 75 kg was used, reflecting the PBPK model's default setting, despite other guidelines suggesting 60 kg (SCCS) (SCCS/1647/22, 2023) and 80 kg (U.S. public health) (Agency for Toxic Substances and Disease Registry and U.S. Department of Health and Human Services PHS, 2023) for adults.

Both kinetic models estimated liver concentrations following intravenous administration of 0.11 mg HCY13, chosen to mimic systemic absorption from the scalp application over a 168-h (7-day) period. The compartmental model predicted the $C_{max\ liver}$ to be 4 pM, while the PBPK model predicted concentrations of **15 pM**. These concentrations were calculated with renal clearance set to zero based on HCY13's ECCS classification (Table 2), yielding a narrow range under both models by exploring various liver metabolism clearance types.

3.5. Mode of action (MoA) hypothesis generation

Based on the data gathered so far, we hypothesized that HCY13 may pose a concern for liver toxicity. To further substantiate this hypothesis, an extra WoE analysis was conducted by identifying 27 analogs of HCY13 with a Tanimoto coefficient exceeding 0.8 using the GenRA software from EPA (U.S Environmental Protection Agency) (Schultz and Cronin, 2017; Cronin et al., 2017). The structural alerts of these analogs were then assessed using the HESS within the OECD QSAR Toolbox. Notably, 21 of these analogs triggered a flutamide hepatotoxicity alert, similar to the warning observed with HCY13 itself (Supplementary Material 2). Considering the structural resemblance of these analogs and the consistent patterns observed, it is reasonable to assume that HCY13 carries a general risk of liver toxicity.

Furthermore, we hypothesized liver steatosis as the mode of action (MoA). This hypothesis builds on the earlier discussion of the CF_3 group in HCY13, which is similar to PFAS compounds that disrupt lipid metabolism, induce oxidative stress, and impair fatty acid β-oxidation, leading to lipid accumulation in hepatocytes—a hallmark of steatosis. The CF_3 group may contribute to these effects through potential PPARA activation, disturbances in the lipolysis-lipogenesis balance, and depletion of liver glutathione levels, as discussed earlier in the context of PFAS exposure (Zhao et al., 2023; Zhang et al., 2023; Sadrabadi et al., 2024; Chen et al., 2020; Khan et al., 2023; Hyötyläinen et al., 2021; Lu et al., 2019; India-Aldana et al., 2023; Ojo et al., 2021; David et al., 2023; Goodrich et al., 2023; Hara and Zeng).

Tier 2: Bioactivity Characterization.

3.6. Targeted testing using a human-relevant test system in vitro

Following the MoA hypothesis and guided by a mechanistically anchored AOP approach (Verhoeven et al., 2024), we subsequently evaluated the steatotic activity of HCY13 using a human *in vitro* stem cell-derived hepatic model (hSKP-HPC), previously shown to be capable of detecting steatotic compounds (Buyl et al., 2023; Rodrigues et al., 2014, 2016; Boeckmans et al., 2021; Natale et al., 2018). Human

skin-derived precursors (hSKP) were isolated from postnatal foreskin samples of young boys (Supplementary Material 3) (Rodrigues et al., 2016; De Kock et al., 2011; De Kock et al., 2012; Escher et al., 2020; Neutral Red Uptake Assay SCOPE, 2022; Verhoeven et al., 2024). The cells were differentiated into hepatocyte-like cells (hSKP-HPC) through a sequential process completed by day 24 and subsequently used for exposure experiments (Rodrigues et al., 2014; De Kock et al., 2011, 2012). Cells were exposed daily to various sub-cytotoxic concentrations of HCY13 over 72 h (Supplementary Material 4) (Escher et al., 2020; Neutral Red Uptake Assay SCOPE, 2022). NaVPA and solvent (media) were positive and negative controls, respectively. We evaluated the expression of eleven marker genes in lipid metabolism derived from Verhoeven et al. (2024). The selected genes represent the MIE, such as *PPARG* and *PPARA* (regulate fatty acid metabolism), *AHR (*regulate xenobiotic metabolism), and *LXRA* (cholesterol metabolism). Additionally, we included genes related to downstream KEs like *CPT1A* (mitochondrial β-oxidation), *CD36* (Fatty Acid (FA) uptake), *SCD1* (FA synthesis), and *FASN* (FA synthesis). We also examined *ACOX1* (mitochondrial β-oxidation), *DGAT2* (FA synthesis), and *APOB* (Very-Low-Density-Lipoprotein (VLDL) export), covering key processes in FA β-oxidation, *de novo lipogenesis*, and lipid export, respectively. These selections align with the KEs of steatosis as outlined by the latest AOP network (Fig. 2). Furthermore, we assessed the accumulation of lipids, which serves as the phenotypic hallmark and a crucial key event in the development of steatosis. Details of the gene expression assay, microscopic imaging of neutral lipids, flow cytometric analysis, and triglyceride (TG) quantification are described in Supplementary Material 5.

Microscopic images revealed that rising concentrations of HCY13 were associated with increased neutral lipid accumulation (Fig. 3A). Flow cytometry semi-quantitatively confirmed this, and a colorimetric assay demonstrated a proportional increase in TG levels with higher HCY13 concentrations (Fig. 3B and C). To understand the mechanism behind lipid accumulation, we investigated the expression of key genes involved in lipid metabolism. Exposure to HCY13 resulted in significant upregulation of *PPARG* and downregulation of *CD36*. *PPARG*, identified as an MIE in the AOP, is a key regulator of lipid metabolism, promoting FA uptake, TG synthesis, and lipid storage. The observed HCY13-mediated upregulation of *DGAT2* expression further contributes to increased TG synthesis and accumulation in hepatocytes, leading to steatosis (Cheol et al., 2007; Monetti et al., 2007; Villanueva et al., 2009).

3.7. Biokinetic refinement (population estimation, metabolites)

3.7.1. Population estimation

Liver concentrations were estimated at both individual and population levels, using deterministic estimation for individuals (Step 3.4) and a probabilistic approach for the population level using GastroPlus 9.9's population simulator with Monte Carlo simulations. This approach incorporated physiological and pharmacokinetic variability by generating virtual subjects with random adjustments to parameters such as gastrointestinal transit times, pH levels, and pharmacokinetic metrics. A cohort of 100 individuals (80% female, 20% male, aged 20–70) was selected using Population Estimates for Age-Related (PEAR) Physiology, allowing a comprehensive assessment using both compartmental and customized PBPK models. Under the assumed exposure scenario and simulation parameters (7 days), the compartmental kinetic model showed no significant difference in $C_{max\ liver}$ values across the different liver metabolism settings, with all simulations consistently predicting a $C_{max\ liver}$ value of 5 pM. In contrast, the PBPK model showed variability

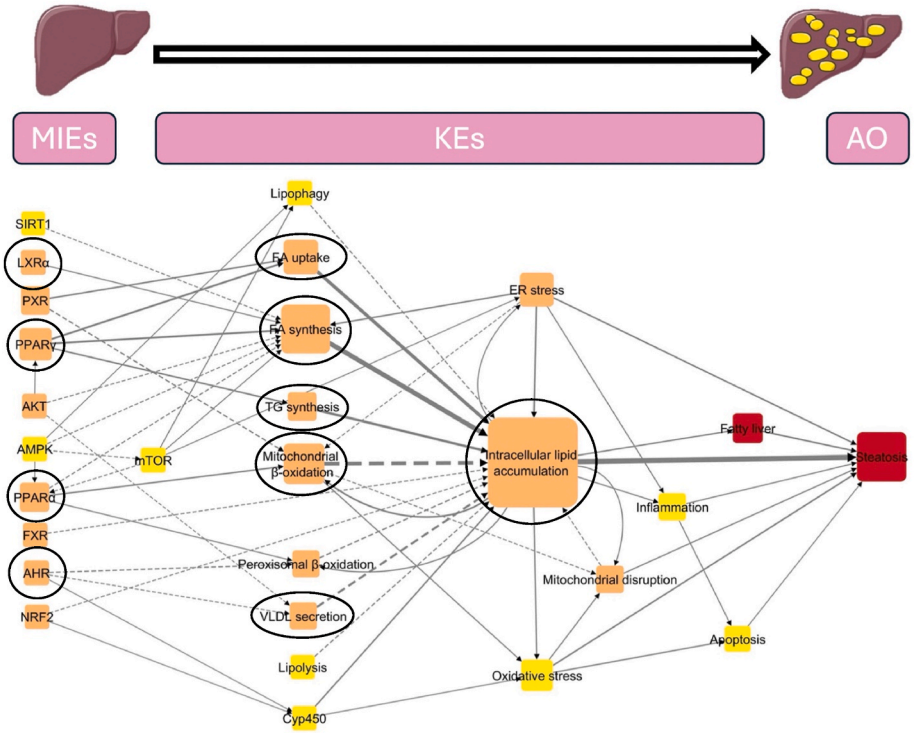

Fig. 2. AOP network applied to evaluate the steatogenic potential of HCY13 using mechanistically-anchored assays (indicated with black-colored ring). Key MIEs, such as the activation of PPARG, PPARA, AHR, and LXRA, are linked to downstream Key Events (KEs), including CD36-mediated fatty acid uptake, FASN and SCD1-driven fatty acid synthesis, ACOX1 and CPT1A-mediated β-oxidation, and DGAT2-regulated triglyceride synthesis. These molecular and cellular mechanisms culminate in the Adverse Outcome (AO) of steatosis, characterized by intracellular lipid accumulation and phenotypic hallmarks like inflammation, mitochondrial disruption, and oxidative stress (Verhoeven et al., 2024). [AOP: Adverse Outcome Pathway, MIEs: Molecular Initiating Events, KEs: Key Events, SIRT1: Sirtuline 1, LXRA: Liver X receptor alpha, PXR: Pregnane X receptor, PPARG: Peroxisome proliferator-activated receptor gamma, AKT: RAC-alpha serine/threonine-protein kinase, AMPK: AMP-activated protein kinase, PPARA: Peroxisome proliferator-activated receptor alpha, FXR: Farnesoid x receptor, AHR: Aryl hydrocarbon receptor, NRF2: Nuclear factor erythroid 2-related factor 2, mTOR: Mechanistic Target Of Rapamycin Kinase.

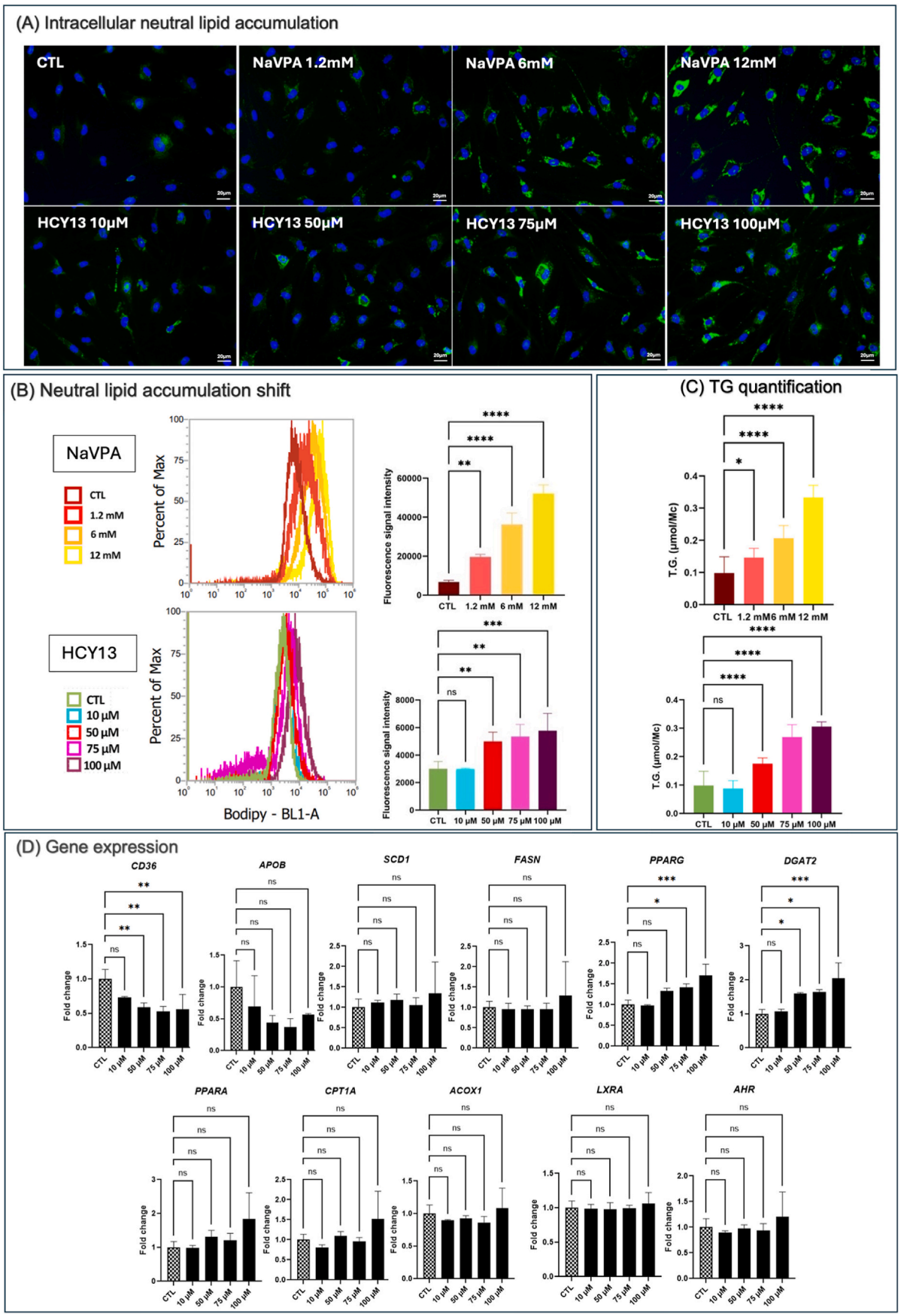

(caption on next page)

Fig. 3. Assessment of lipid accumulation in the hSKP-HPC model upon HCY13 exposure was performed using multiple assays. (A) Microscopy depicts cells treated with HCY13, a solvent control and the positive control NaVPA. Blue staining represents the nuclei, and green staining indicates neutral lipids (Boeckmans et al., 2021). (B) Flow cytometry shows increasing Bodipy 493/503 signal intensity with rising HCY13 concentrations. Adjacent, signal intensity is plotted against concentrations (n = 4) (Boeckmans et al., 2020). (C) Colorimetric TG quantification reveals a trend of increasing TG concentration at higher HCY13 concentrations (n = 3) (Elabscience.com). (D) Gene expression analysis of HCY13 focuses on key genes representing CD36 (uptake of lipids), APOB (export of lipids), ACOX1 and CPT1A (beta-oxidation), FASN, SCD1, and DGAT2 (*de novo* lipogenesis), as well as PPARA, PPARG, LXRA, and AHR (molecular initiating events, or MIEs) highlighting significant DGAT2, CD36, and PPARG gene up or down-regulation (Rodrigues et al., 2014). For all graphs, statistical significance was determined using one-way ANOVA and Tukey's or Dunnett's tests (*$p < 0.05$), with error bars representing the variability across three independent runs, each with two technical replicates. [CTL: negative control condition, TG: Triglycerides, AHR: Aryl hydrocarbon receptor, PPARA: Peroxisome proliferator-activated receptor alpha, PPARG: Peroxisome proliferator-activated receptor gamma, APOB: Apolipoprotein B, ACOX1: Acyl-coenzyme A oxidase 1, CD36: Cluster of differentiation 36, FASN: Fatty acid synthase, SCD1: Stearoyl-CoA desaturase-1, CPT1A: Carnitine palmitoyltransferase 1A, DGAT2: Diacylglycerol O-acyltransferase 2, LXRA: Liver X receptor alpha.].

among the three liver metabolism settings (hepatocytes, microsomes, and CYP450 enzymes). Specifically, the PBPK model estimated a $C_{max\ liver}$ value of 20 pM with both CYP450 enzyme metabolism and microsomes, while predicting 10 pM with hepatocytes.

3.7.2. Metabolites refinement

All three metabolites of HCY13 were analyzed for repeated dose liver toxicity using HESS via the OECD QSAR toolbox. The analysis revealed that M1 and M2 triggered a flutamide-hepatotoxicity alert, while M3 showed no structural alert by HESS. Per the iTTC principle, potential health risks of hepatotoxicity-alert metabolites M1 and M2 were assessed. Assuming the complete metabolism of HCY13 into M1 (74%) and M2 (26%) within the liver, their plasma concentrations were estimated using GastroPlus 9.9 in both single-object and population models. The formation of metabolite M1 from 0.11 mg of HCY13 was **0.081 mg,** while that of metabolite M2 was **0.029 mg**, based on the respective 74% and 26% metabolism rates. The results indicated that the maximum plasma concentrations ($C_{max\ plasma}$) of M1 in the compartmental model was 3 pM at the individual level and 4 pM at the population level. In contrast, in the PBPK model, the maximum plasma concentrations were 90 pM at the individual level and 100 pM at the population simulation level. For M2, the $C_{max\ plasma}$ in the compartmental model was 0.5 pM at the individual level and 0.8 pM at the population level. According to the PBPK model, the $C_{max\ plasma}$ for M2 was estimated at 40 pM for individual-level simulations and 50 pM for population-level simulations. These concentrations are well below the iTTC threshold of 1 μM, suggesting that neither metabolite M1 nor metabolite M2 is likely to induce significant biological effects. Therefore, the focus of the risk assessment from this step was on the parent compound HCY13 (SCCS/1647/22, 2023; Blackburn et al., 2020).

3.8. Points of Departure calculation using the BMC approach (PoD_{NAM})

The concentration-response curves for TG accumulation and those showing significant changes in gene expression (*DGAT2*, *PPARG*, and *CD36*) were analyzed using the Benchmark Concentration (BMC) approach in PROAST 70.1 software by RIVM (Rijksinstituut voor Volksgezondheid en Milieu). This method estimates the exposure level that causes a predefined change, known as the Benchmark Response (BMR), leveraging full dose-response data and various statistical models for robust risk estimation. A BMR of 20% was applied for lipid accumulation, corresponding to one standard deviation (SD) of the control group, aligning with EPA guidelines (US EPA, 2016). For gene expression, due to higher variability (SD 0.01 to 0.1), a BMR of 50% was set to capture meaningful changes (Fortin et al., 2023; Fragki et al., 2023). Each analysis generated a BMC confidence interval, with the lowest (BMC_L) and highest (BMC_U) estimates, designating the BMC_L as the PoD_{NAM} for each biomarker (Middleton et al., 2022). *DGAT2* had a BMC_L range of 27.8–67.9 μM, *PPARG* showed 57.8–92.2 μM, and *CD36* ranged 44.8–555.0 μM, indicating varying sensitivities to HCY13. TG accumulation, the most sensitive biomarker, showed the lowest BMC_L of 0.484 μM, emphasizing its central role in the AOP of steatosis (Luckert et al., 2018; Vinken, 2015; Svingen et al., 2021). This comprehensive analysis is visually represented using exponential and Hill models in Supplementary Material 6.

Tier 3 – Risk characterization.

3.9. Calculation of Bioactivity-Exposure Ratio (BER) based on lowest PoD_{NAM}

The Bioactivity Exposure Ratio (BER) method assesses safety by comparing the most sensitive *in vitro* bioactivity threshold (PoD_{NAM}) with predicted human exposure levels, specifically $C_{max\ liver}$. A BER above 1 indicates that the bioactivity threshold is higher than the estimated internal exposure level, providing a margin of safety. Conversely, a BER below 1 suggests potential adverse effects, warranting further investigation (Health Canada, 2021). Using the PoD_{NAM} of 0.484 μM derived from TG accumulation, we calculated the BER by dividing this value by the $C_{max\ liver}$ predicted by GastroPlus 9.9. In the compartmental model, single-object simulation yielded a $C_{max\ liver}$ value of 4 pM, resulting in a BER of 121000. Population simulation resulted in a $C_{max\ liver}$ concentration of 5 pM, with a corresponding BER of 96800. For the PBPK model, single-object simulation produced a $C_{max\ liver}$ concentration of **15 pM**, leading to a BER of 32267. Population-based simulation, depending on liver metabolism settings, resulted in $C_{max\ liver}$ values of 10 pM and 20 pM, with BER values of 48400 and 24200, respectively. As all BER values are much higher than 1, no significant risk of liver steatosis is expected under the assumed use conditions of HCY13, based on the tools and test system applied in the assessment.

3.10. Risk evaluation and uncertainties assessment

Accurately documenting uncertainties in data generation is a critical step within the NGRA framework. While quantifying uncertainties is ideal, it is often not feasible. To address this, we employed a qualitative approach, classifying certainties as Low (L), Medium (M), or High (H) to capture potential variability and biases in the assessment. Transparent documentation of *in silico* and *in vitro* model limitations is essential for fostering trust and improving the adoption of NGRA methodologies. Table 3 provides a qualitative assessment of uncertainties, detailing the level of certainty in each area, potential reasons for over- or underestimations, and the possible impact on overall risk assessment (Dent et al., 2021; Gosling, 2013). Key areas, such as internal exposure and biological coverage, have been extensively discussed in the literature, underscoring the importance of accurate PBPK modeling (Moxon et al., 2020) and comprehensive biological coverage (Carmichael et al., 2022) for reliable risk assessments with animal-free approaches.

Although HCY13 is unlikely to induce steatosis under the assumed use conditions at both individual and population levels, understanding the key parameters influencing $C_{max\ liver}$ remains crucial for risk assessment. To evaluate the confidence in our findings, we conducted a sensitivity analysis on 16 parameters affecting $C_{max\ liver}$, systematically examining how changes in these key model input parameters impact the model output (EMA, 2018). Our findings identified dose and LogD as primary drivers, followed by the liver partition coefficient (Kp). Factors such as Rbp, Fup, and liver clearance significantly contributed to

Table 3
Qualitative evaluation of certainty levels encountered in our animal-free NGRA workflow for assessing the liver steatogenic risk of 2.5% (w/w) HCY13 in non-oxidative hair coloring products. SCCS NoG: Scientific Committee on Consumer Safety Notes of Guidance, PoD: Point of Departure.

Area of uncertainty	Level of certainty	Rationale of the over or under-estimation of the value	Impact on risk assessment decision
Consumer exposure	High: • Consumer habits and practices derived from SCCS/1647/22 • Regulatory maximum of 2.5% usage in non-oxidative hair coloring products	Overestimation (the maximum use is likely to be an overestimate)	More conservative
Toxicity identification	Medium: • Based on *in silico* structural alerts within the applicability domain • Consideration of functional groups in the assessment	Overestimation	Increase decision certainty
Metabolites identification	Low: • *In silico* data analysis within the applicability domain	Underestimation	Decrease decision certainty
Internal exposure	Medium: • ADME parameters predicted through *in silico* tools within the applicability domain • Sensitivity analysis conducted to quantify the influence of input parameters on model output • Characterization of inter-individual differences in single-object and population $C_{max\ liver}$ using deterministic and probabilistic approaches	Reasonable worst case	More conservative
Range of biomarkers assessed	Medium: • Moderate biological coverage	Moderate coverage	Increase uncertainty
In vitro tests	Medium: • Short-term repeated exposure conducted in a human-relevant test system	Protective enough	No impact
PoD selection	High: • Four BMC_L ranging from 0.484 to 57.8 μM, with the lowest one selected as the most sensitive	Unlikely to be overestimation	Increase confidence

variations, and individual-specific parameters, particularly body weight, were crucial in determining variability in $C_{max\ liver}$.

4. Discussion

Traditional risk assessment relies heavily on animal testing to identify toxicity thresholds, a method that, despite its comprehensiveness, faces ethical concerns, high costs, and potential inaccuracies due to intra- and interspecies differences. With the EU ban on animal testing for cosmetics, the NGRA approach has emerged as a viable alternative, focusing on exposure-led, hypothesis-driven, human-relevant, and harm-prevention principles (Dent et al., 2018; Gwinn et al., 2017; Browne et al., 2024; Schmeisser et al., 2023). Human-based NAMs are central to NGRA because they offer more precise data on how chemicals affect the human body. By integrating into mechanistic frameworks like AOPs, they help ensure these methods meet the standards of traditional risk assessments. This alignment strengthens scientific evaluations, ultimately aiding regulatory acceptance of these approaches (Bajard et al., 2023; Hoffmann et al., 2022; Bonneau et al., 2021). Case studies utilizing scientifically valid animal-free methods are essential for gaining regulatory acceptance of NGRA methodologies by demonstrating their reliability and effectiveness in protecting human health (Dent et al., 2021; Rogiers et al., 2020). However, robust strategies are necessary to address uncertainties in the generated *in vitro* data and computational predictions, including ADME and PBPK modeling (Brescia et al., 2023).

HCY13 was selected for this NGRA case study due to its prior identification as a potentially hepatotoxic cosmetic ingredient from 90-day repeated-dose animal studies (Gustafson et al., 2020). Flagged four times for hepatotoxicity by a combination of mechanistic and statistical *in silico* tools, this underscores the need for integrating both approaches to enhance confidence in hazard identification (Teixeira do Amaral et al., 2014). Despite these flags, the SCCS's traditional risk assessment deems HCY13 safe for use as both an oxidative and non-oxidative hair dye, with a maximum on-head concentration of 2.5% (w/w) (). Selecting a compound with historical data is essential for validating NGRA, as it allows comparisons between NAM-based assessments and traditional risk assessments, demonstrating how to analyze, integrate, and interpret these data effectively.

This study utilized an OECD 428 *in vitro* dermal absorption study under non-oxidative conditions, revealing a dermal bioavailability of 0.13 % of the applied dose (). This corresponds to an internal dose of 0.11 mg, irrespective of the body weight considered in the exposure scenario. The use of OECD 428 data ensures a reliable margin of safety, as it is based on actual tested conditions rather than hypothetical worst-case scenarios. In the absence of *in vitro* dermal bioavailability data, *in silico* tools, such as the Skin Permeation Calculator—which does not require formulation-specific parameters—, or the TCAT model from GastroPlus, which relies on formulation-specific data, can be used to estimate dermal bioavailability (Kuster et al., 2022; Tsakalozou et al., 2023; Spires, 2020; DumontCoralie and AsturiolDavid; van Osdol et al., 2024).

Liver concentration estimates for HCY13 required additional ADME parameters predicted by ADMET Predictor® 11.0, increasing uncertainty in organ-level concentrations (Dulsat et al., 2023; Zhai et al., 2022; Yamashita and Hashida, 2004). Using GastroPlus® 9.9, we employed a compartmental model and a customized PBPK model to estimate liver concentrations, assuming an IV administration of the calculated internal dose of 0.11 mg for an individual of 75 kg, simulated over 7 days. While generic kinetic models are generally accurate enough for organ concentration estimates, PBPK models provide enhanced flexibility and refinement for NAM-based risk assessments (EPA, 2018; Punt et al., 2022; Deepika and Kumar, 2023). Probabilistic modeling at the population level was used to bridge this gap to refine exposure estimates from worst-case to more realistic scenarios, enhancing confidence in risk assessment decisions (Tozer et al., 2023; Chiu and Rusyn, 2018). While investigating internal exposure at the population level increases confidence in risk assessment decision-making (Chiu and Rusyn, 2018), identifying metabolites via *in silico*-only methods heightens uncertainty, as reflected in the low certainty level associated with the iTTC approach. Increased confidence would be achieved if metabolites were experimentally determined *in vitro*, providing more accurate and reliable data to inform the risk assessment process. Although shown to be capable of detecting steatotic compounds (Buyl et al., 2023; Rodrigues et al., 2014, 2016; Boeckmans et al., 2021; Natale et al., 2018), the limited metabolic capacity of the hSKP-HPC cells used for bioactivity characterization necessitated reliance on *in silico* methods for metabolite identification. This limitation of the test system was addressed by demonstrating that the predicted plasma concentrations of the M1 and M2 metabolites were below the accepted iTTC threshold of 1 μM (Ebmeyer et al., 2024; SCCS/1647/22, 2023), indicating no significant biological effects.

Consequently, the risk assessment focused on the parent compound

HCY13. To better simulate real-life conditions and further refine the evaluation, plasma protein binding assays, the use of primary human hepatocyte cultures, liver S9 fractions, or microsomes, along with advanced 3D liver models, could be considered (Peeters et al., 2020; N et al., 2023). Additionally, confirming the absence of bioactivity of the M1 and M2 metabolites through *in vitro* testing would also be required.

The study found that HCY13 exposure led to the upregulation of *PPARG* and *DGAT2*, along with the downregulation of *CD36*, highlighting a complex regulatory environment. While *PPARG* typically exacerbates steatosis (Ratziu et al., 2008; Fernández-Miranda et al., 2008; Ahmadian et al., 2013; Tontonoz and Spiegelman, 2008), and *DGAT2* enhances TG synthesis (Yen et al., 2008; Cases et al., 1998, 2001), the downregulation of *CD36*—usually upregulated by PPARγ (Maréchal et al., 2018; Febbraio et al., 2001)—suggests alternative regulatory mechanisms, such as post-transcriptional regulation by microRNAs or HCY13-specific effects that alter normal signaling pathways (Bravo-Ruiz et al., 2021; Niculite et al., 2019; Varga et al., 2011; Pan et al., 2022; Lee et al., 2017). Moreover, the downregulation of *CD36* is likely an adaptive response to intracellular fat accumulation driven by *de novo* lipogenesis, wherein the cell reduces FA uptake to prevent further lipid overload. The response may have differed at earlier time points, potentially exhibiting higher *CD36* expression. This interplay likely drives the lipid accumulation observed, contributing to the steatogenic phenotype despite the altered PPARγ-CD36 relationship. Future studies could explore earlier time points, like 8 h post-exposure, to capture MIE dynamics and clarify the initial regulatory responses to HCY13. This would deepen understanding of early gene expression changes and the mechanisms contributing to steatosis. However, the 72-h findings robustly establish the key regulatory changes linked to HCY13 exposure, providing a solid foundation for risk assessment.

A notable strength of this case study was using the BMC approach across significantly affected biomarkers at both the gene expression and functional levels, particularly TG accumulation—a hallmark of steatosis. Identifying the most sensitive biomarker with the lowest BMC_L for PoD_{NAM} from functional data enhances confidence in the risk assessment (Sand et al., 2006; Yasuhiko et al., 2022), as this approach captures biologically significant effects beyond gene expression changes alone (Burden et al., 2021; Crump et al., 2010).

The overall risk assessment is based on a comparison between the maximum internal liver concentration ($C_{max\ liver}$) and the PoD_{NAM}, derived from the nominal concentration in culture medium. The use of the nominal concentration is justified by the physicochemical properties of HCY13. It is known that parameters such as volatility, solubility, hydrophobicity, and binding to plastic can significantly influence a compound's *in vitro* distribution (Nicol et al., 2024). Among these, the octanol/water partition coefficient (log $P_{o/w}$) is a key determinant, as chemicals with a high log $P_{o/w}$ (>4) tend to significantly bind to plastic, reducing their bioavailable concentration in *in vitro* assays (Henneberger et al., 2021; Nicol et al., 2024). For HCY13, this concern is minimal, given its experimentally measured log $P_{o/w}$ of 2.54 (). Moreover, HCY13 has a very low vapor pressure (Table 2) and a negligible Henry's Law constant (1.54e-5 Pa-m^3/mol, calculated using HENRYWIN v3.21 from EpiSuite, EPA), indicating minimal evaporation. Collectively, these physicochemical characteristics of HCY13 suggest that it remains predominantly in the culture medium, resulting in an actual concentration (C_{free}) that closely approximates the nominal concentration ($C_{nominal}$) (Proença et al., 2021). An even more precise assessment would involve using the intracellular concentration (C_{cell}) from the *in vitro* system, as it better reflects the biologically effective dose. Estimating C_{cell} would, however, require the integration of advanced *in vitro* dosimetry models that account for cellular uptake, binding, and distribution (Bouhifd et al., 2010). Alternatively, the PoD_{NAM} could be compared to predicted concentrations in the plasma supplying the liver ($C_{max\ plasma}$) rather than the $C_{max\ liver}$ (Nicol et al., 2024; Magurany et al., 2023).

A key aspect of NGRA is distinguishing between adaptive and adverse toxicological responses. Steatosis, while not a disease per se, is associated with broader liver toxicity due to lipid accumulation in hepatocytes, which can impair liver function. The NGRA approach in this study estimates bioactivity thresholds that are typically lower and more conservative than adversity thresholds derived from animal studies that measure apical endpoints (Dent et al., 2018; Paul Friedman et al., 2020). The PoD_{NAM} for deriving BERs was based on a functional biomarker assessed after short-term repeated exposure in a human-relevant *in vitro* model. This resulted in a range of significantly high BERs, indicating a substantial margin of safety. A high BER suggests that the bioactivity threshold is well above the estimated human exposure, reducing the need to distinguish between adaptation and adversity. However, when BER values are close to 1, further mechanistic investigation is necessary to determine if observed bioactivity may lead to adverse health effects. In such cases, enhancing the test system's biological coverage—for example, by testing mitochondrial beta-oxidation, mitochondrial disruption, or ER stress, as outlined in the AOP network by Verhoeven et al. (2024)—is essential. This helps to understand the mechanistic involvement of the system better and accurately assess potential risks (Dent et al., 2021; Middleton et al., 2022; Schmeisser et al., 2023; Magurany et al., 2023; Berridge et al., 2024).

This case study employed a WoE approach to assess the MoA, providing a robust, biologically-based framework for evaluating systemic toxicants (Simon et al., 2014; Clewell, 2005; Determining Modes Of Action for, 1999). Our results are consistent with traditional animal-based hazard and risk assessment, which deemed HCY13 safe at a maximum on-head concentration of 2.5% (w/w) (). Importantly, traditional studies did not identify the liver as a target organ in rats after 90-day oral exposure to HCY13. In humans, the primary enzymes involved in the metabolism of HCY13 are CYP1A2 and CYP3A4. While these enzymes have varying metabolic capacity between humans and laboratory animals (Hammer et al., 2021; Abass et al., 2023), no species-specific variation in risk of liver steatosis is found for HCY13.

5. Conclusion

This *ab initio* NGRA of HCY13 for liver steatogenic risk adhered to a protective, conservative approach, gradually refining towards real-world scenarios using probabilistic models and considering the actual versus nominal concentrations in *in vitro* assessments. NAMs provided robust insights into exposure and bioactivity, achieving an overall medium level of certainty. Our findings indicate that HCY13 is unlikely to present significant steatogenic liver toxicity risks under the assumed use conditions, based on the tools and test system applied in the assessment. Continued development and implementation of NAMs are expected to strengthen confidence in non-animal safety assessments and reinforce their increasing role in regulatory decision-making. While there is room for further refinement, this case study underscores the practical applicability of NAMs within a tiered NGRA framework.

CRediT authorship contribution statement

Sara Sepehri: Writing – review & editing, Writing – original draft, Visualization, Software, Resources, Methodology, Investigation, Formal analysis, Data curation, Conceptualization. **Dinja De Win:** Investigation. **Anja Heymans:** Investigation. **Freddy Van Goethem:** Writing – review & editing. **Robim M. Rodrigues:** Writing – review & editing, Visualization, Methodology, Conceptualization. **Vera Rogiers:** Writing – review & editing. **Tamara Vanhaecke:** Writing – review & editing, Validation, Supervision, Methodology, Funding acquisition, Conceptualization.

Declaration of generative AI and AI-assisted technologies in the writing process

During the preparation of this work, the author(s) used ChatGPT in order to edit and improve English sentencing. After using this tool/

service, the author(s) reviewed and edited the content as needed and take(s) full responsibility for the content of the publication.

Funding

This work was supported by the Onderzoeksraad Vrije Universiteit Brussel (TOXIN project), the Research Chair Mireille Aerens on developing Alternatives to Animal Testing and the Partnership for the Assessment of Risk from Chemicals (PARC), funded by the European Union's Horizon Europe research and innovation program under Grant Agreement No 101057014.

Declaration of competing interest

The authors declared no potential conflicts of interest regarding this article's research, authorship, and/or publication.

Acknowledgments

The authors would like to express their gratitude to Simulation Plus® for granting access to ADMET Predictor 11 and GastroPlus 9.9, which were instrumental in this study's computational modeling aspects. Special thanks also go to M. Zarr for their contribution to Fig. 1, which enhanced the visual presentation of our framework.

Appendix A. Supplementary data

Supplementary data to this article can be found online at https://doi.org/10.1016/j.yrtph.2025.105794.

Data availability

Data will be made available on request.

References

Abass, K., Reponen, P., Anyanwu, B., Pelkonen, O., 2023. Inter-species differences between humans and other mammals in the in vitro metabolism of carbofuran and the role of human CYP enzymes. Environ. Toxicol. Pharmacol. 102, 104243. https://doi.org/10.1016/J.ETAP.2023.104243.

Agency for Toxic Substances and Disease Registry, U.S. Department of Health and Human Services PHS, 2023. Exposure dose guidance for body weight. Exposure Dose Guidance for Body Weight.

Ahmadian, M., Suh, J.M., Hah, N., Liddle, C., Atkins, A.R., Downes, M., et al., 2013. PPARγ signaling and metabolism: the good, the bad and the future. Nat. Med. 19, 557–566. https://doi.org/10.1038/NM.3159.

Assaf Vandecasteele, H., Gautier, F., Tourneix, F., Vliet, E van, Bury, D., Alépée, N., 2021. Next generation risk assessment for skin sensitisation: a case study with propyl paraben. Regul. Toxicol. Pharmacol. 123, 104936. https://doi.org/10.1016/J.YRTPH.2021.104936.

Bajard, L., Adamovsky, O., Audouze, K., Baken, K., Barouki, R., Beltman, J.B., et al., 2023. Application of AOPs to assist regulatory assessment of chemical risks – case studies, needs and recommendations. Environ. Res. 217, 114650. https://doi.org/10.1016/J.ENVRES.2022.114650.

Baltazar, M.T., Cable, S., Carmichael, P.L., Cubberley, R., Cull, T., Delagrange, M., et al., 2020. A next-generation risk assessment case study for coumarin in cosmetic products. Toxicol. Sci. 176, 236–252. https://doi.org/10.1093/TOXSCI/KFAA048.

Berggren, E., White, A., Ouedraogo, G., Paini, A., Richarz, A.N., Bois, F.Y., et al., 2017. Ab initio chemical safety assessment: a workflow based on exposure considerations and non-animal methods. Comput. Toxicol. 4, 31. https://doi.org/10.1016/J.COMTOX.2017.10.001.

Berridge, B.R., Bucher, J.R., Sistare, F., Stevens, J.L., Chappell, G.A., Clemons, M., et al., 2024. Enabling novel paradigms: a biological questions-based approach to human chemical hazard and drug safety assessment. Toxicol. Sci. 198, 4–13. https://doi.org/10.1093/TOXSCI/KFAD124.

Bhatt, S., Dhiman, S., Kumar, V., Gour, A., Manhas, D., Sharma, K., et al., 2022. Assessment of the CYP1A2 inhibition-mediated drug interaction potential for pinocembrin using in silico, in vitro, and in vivo approaches. ACS Omega 7, 20321–20331. https://doi.org/10.1021/ACSOMEGA.2C02315/SUPPL_FILE/AO2C02315_SI_001.PDF.

Bialas, I., Zelent-Kraciuk, S., Jurowski, K., 2023. The skin sensitisation of cosmetic ingredients: review of actual regulatory status. Toxics 11. https://doi.org/10.3390/TOXICS11040392.

Blackburn, K.L., Carr, G., Rose, J.L., Selman, B.G., 2020. An interim internal Threshold of Toxicologic Concern (iTTC) for chemicals in consumer products, with support from an automated assessment of ToxCast™ dose response data. Regul. Toxicol. Pharmacol. 114, 104656. https://doi.org/10.1016/J.YRTPH.2020.104656.

Boeckmans, J., Natale, A., Rombaut, M., Buyl, K., Vanhaecke, T., Rogiers, V., et al., 2020. Flow cytometric quantification of neutral lipids in a human skin stem cell-derived model of NASH. MethodsX 7. https://doi.org/10.1016/J.MEX.2020.101068.

Boeckmans, J., Natale, A., Rombaut, M., Buyl, K., Cami, B., De Boe, V., et al., 2021. Human hepatic in vitro models reveal distinct anti-NASH potencies of PPAR agonists. Cell Biol. Toxicol. 37, 293–311. https://doi.org/10.1007/S10565-020-09544-2.

Bonneau, N., Baudouin, C., Brignole-Baudouin, F., 2021. AOP and IATA applied to ocular surface toxicity. Regul. Toxicol. Pharmacol. 125, 105021. https://doi.org/10.1016/J.YRTPH.2021.105021.

Bouhifd, M., Mennecozzi, M., Rodrigues, R., Zaldívar, J.M., 2010. A Biology-Based Dynamic Approach for the Modelling of Toxicity in Cell-Based Assays. OPOCE.

Bravo-Ruiz, I., Medina, M.Á., Martínez-Poveda, B., 2021. From food to genes: transcriptional regulation of metabolism by lipids and carbohydrates. Nutrients 13. https://doi.org/10.3390/NU13051513.

Brescia, S., Alexander-White, C., Li, H., Cayley, A., 2023. Risk assessment in the 21st century: where are we heading? Toxicol Res (Camb) 12, 1. https://doi.org/10.1093/TOXRES/TFAC087.

Browne, P., Paul Friedman, K., Boekelheide, K., Thomas, R.S., 2024. Adverse effects in traditional and alternative toxicity tests. Regul. Toxicol. Pharmacol. 148, 105579. https://doi.org/10.1016/J.YRTPH.2024.105579.

Burden, N., Clift, M.J.D., Jenkins, G.J.S., Labram, B., Sewell, F., 2021. Opportunities and challenges for integrating new in vitro methodologies in hazard testing and risk assessment. Small 17, 2006298. https://doi.org/10.1002/SMLL.202006298.

Bury, D., Head, J., Keller, D., Klaric, M., Rose, J., 2021a. The Threshold of Toxicological Concern (TTC) is a pragmatic tool for the safety assessment: case studies of cosmetic ingredients with low consumer exposure. Regul. Toxicol. Pharmacol. 123. https://doi.org/10.1016/J.YRTPH.2021.104964.

Bury, D., Alexander-White, C., Clewell, H.J., Cronin, M., Desprez, B., Detroyer, A., et al., 2021b. New framework for a non-animal approach adequately assures the safety of cosmetic ingredients – a case study on caffeine. Regul. Toxicol. Pharmacol. 123, 104931. https://doi.org/10.1016/J.YRTPH.2021.104931.

Buyl, K., Vrints, M., Fernando, R., Desmae, T., Van Eeckhoutte, T., Jans, M., et al., 2023. Human skin stem cell-derived hepatic cells as in vitro drug discovery model for insulin-driven de novo lipogenesis. Eur. J. Pharmacol. 957, 175989. https://doi.org/10.1016/J.EJPHAR.2023.175989.

Carmichael, P.L., Baltazar, M.T., Cable, S., Cochrane, S., Dent, M., Li, H., et al., 2022. Ready for regulatory use: NAMs and NGRA for chemical safety assurance. ALTEX 39, 359–366. https://doi.org/10.14573/altex.2204281.

Cases, S., Smith, S.J., Zheng, Y.W., Myers, H.M., Lear, S.R., Sande, E., et al., 1998. Identification of a gene encoding an acyl CoA:diacylglycerol acyltransferase, a key enzyme in triacylglycerol synthesis. Proc. Natl. Acad. Sci. U. S. A. 95, 13018. https://doi.org/10.1073/PNAS.95.22.13018.

Cases, S., Stone, S.J., Zhou, P., Yen, E., Tow, B., Lardizabal, K.D., et al., 2001. Cloning of DGAT2, a second mammalian diacylglycerol acyltransferase, and related family members. J. Biol. Chem. 276, 38870–38876. https://doi.org/10.1074/JBC.M106219200.

Chan, R., Benet, L.Z., 2018. Measures of BSEP inhibition in vitro are not useful predictors of DILI. Toxicol. Sci. 162, 499. https://doi.org/10.1093/TOXSCI/KFX284.

Chen, B., Om Abuassba, A., 2021. Compartmental models with application to pharmacokinetics. Procedia Comput. Sci. 187, 60–70. https://doi.org/10.1016/j.procs.2021.04.033.

Chen, Z., Yang, T., Walker, D.I., Thomas, D.C., Qiu, C., Chatzi, L., et al., 2020. Dysregulated lipid and fatty acid metabolism link perfluoroalkyl substances exposure and impaired glucose metabolism in young adults. Environ. Int. 145, 106091. https://doi.org/10.1016/J.ENVINT.2020.106091.

Cheol, S.C., Savage, D.B., Kulkarni, A., Xing, X.Y., Liu, Z.X., Morino, K., et al., 2007. Suppression of diacylglycerol acyltransferase-2 (DGAT2), but not DGAT1, with antisense oligonucleotides reverses diet-induced hepatic steatosis and insulin resistance. J. Biol. Chem. 282, 22678–22688. https://doi.org/10.1074/JBC.M704213200.

Chiu, W.A., Rusyn, I., 2018. Advancing chemical risk assessment decision-making with population variability data: challenges and opportunities. Mamm. Genome 29, 182. https://doi.org/10.1007/S00335-017-9731-6.

Clewell, H., 2005. Use of mode of action in risk assessment: past, present, and future. Regul. Toxicol. Pharmacol. 42, 3–14. https://doi.org/10.1016/J.YRTPH.2005.01.008.

Cronin, M.T.D., Enoch, S.J., Mellor, C.L., Przybylak, K.R., Richarz, A.N., Madden, J.C., 2017. In silico prediction of organ level toxicity: linking chemistry to adverse effects. Toxicol. Res. 33, 173–182. https://doi.org/10.5487/TR.2017.33.3.173.

Cronin, M.T.D., Ball, N., Beken, S., Bender, H., Bercaru, O., Caneva, L., et al., 2023. Exposure considerations in human safety assessment: report from an EPAA Partners' Forum. Regul. Toxicol. Pharmacol. 144. https://doi.org/10.1016/j.yrtph.2023.105483.

Crump, K.S., Chen, C., Louis, T.A., 2010. The future use of in vitro data in risk assessment to set human exposure standards: challenging problems and familiar solutions. Environ. Health Perspect. 118, 1350. https://doi.org/10.1289/EHP.1001931.

David, N., Antignac, J.P., Roux, M., Marchand, P., Michalak, S., Oberti, F., et al., 2023. Associations between perfluoroalkyl substances and the severity of non-alcoholic fatty liver disease. Environ. Int. 180, 108235. https://doi.org/10.1016/J.ENVINT.2023.108235.

Deepika, D., Kumar, V., 2023. The role of "physiologically based pharmacokinetic model (PBPK)" new approach methodology (NAM) in pharmaceuticals and environmental

chemical risk assessment. Int. J. Environ. Res. Publ. Health 20. https://doi.org/10.3390/IJERPH20043473. Page 3473 2023;20:3473.
Dent, M., Amaral, R.T., Da Silva, P.A., Ansell, J., Boisleve, F., Hatao, M., et al., 2018. Principles underpinning the use of new methodologies in the risk assessment of cosmetic ingredients. Comput. Toxicol. 7, 20–26. https://doi.org/10.1016/j.comtox.2018.06.001.
Dent, M.P., Vaillancourt, E., Thomas, R.S., Carmichael, P.L., Ouedraogo, G., Kojima, H., et al., 2021. Paving the way for application of next generation risk assessment to safety decision-making for cosmetic ingredients. Regul. Toxicol. Pharmacol. 125, 105026. https://doi.org/10.1016/J.YRTPH.2021.105026.
Determining Modes of Action for Biologically Based Risk Assessments, 1999.
Directorate, E., Committee, B., 2021. Case Study on Use of an Integrated Approach for Testing and Assessment (IATA) for Systemic Toxicity of Phenoxyethanol when Included at 1% in a Body Lotion.
Dulsat, J., López-Nieto, B., Estrada-Tejedor, R., Borrell, J.I., 2023. Evaluation of free online ADMET tools for academic or small biotech environments. Molecules 28, 776. https://doi.org/10.3390/MOLECULES28020776/S1.
DumontCoralie, PrietoPilar, AsturiolDavid, WorthAndrew. Review of the Availability of In Vitro and In Silico Methods for Assessing Dermal Bioavailability. Https://HomeLiebertpubCom/Aivt 2015;1:147–164. https://doi.org/10.1089/AIVT.2015.0003.
Ebmeyer, J., Najjar, A., Lange, D., Boettcher, M., Voß, S., Brandmair, K., et al., 2024. Next generation risk assessment: an ab initio case study to assess the systemic safety of the cosmetic ingredient, benzyl salicylate, after dermal exposure. Front. Pharmacol. 15. https://doi.org/10.3389/FPHAR.2024.1345992.
Elabscience.com. Triglyceride (TG) colorimetric assay kit (Single Reagent, GPO-PAP Method) E-BC-K261-M, 1–12.
EMA, 2018. Committee for Medicinal Products for Human Use (CHMP) Guideline on the Reporting of Physiologically Based Pharmacokinetic (PBPK) Modelling and Simulation.
EPA, 2018. PHYSIOLOGICALLY-BASED pharmacokinetic (PBPK) models. https://doi.org/10.1093/toxsci/kfm100.
Escher, B.I., Henneberger, L., König, M., Schlichting, R., Fischer, F.C., 2020. Cytotoxicity burst? Differentiating specific from nonspecific effects in tox21 in vitro reporter gene assays. Environ. Health Perspect. 128, 1–10. https://doi.org/10.1289/EHP6664.
Febbraio, M., Hajjar, D.P., Silverstein, R.L., 2001. CD36: a class B scavenger receptor involved in angiogenesis, atherosclerosis, inflammation, and lipid metabolism. J. Clin. Investig. 108, 785–791. https://doi.org/10.1172/JCI14006.
Fernández-Miranda, C., Pérez-Carreras, M., Colina, F., López-Alonso, G., Vargas, C., Solís-Herruzo, J.A., 2008. A pilot trial of fenofibrate for the treatment of non-alcoholic fatty liver disease. Dig. Liver Dis. 40, 200–205. https://doi.org/10.1016/J.DLD.2007.10.002.
Fortin, A.M.V., Long, A.S., Williams, A., Meier, M.J., Cox, J., Pinsonnault, C., et al., 2023. Application of a new approach methodology (NAM)-based strategy for genotoxicity assessment of data-poor compounds. Front. Toxicol. 5. https://doi.org/10.3389/FTOX.2023.1098432/FULL.
Fragki, S., Louisse, J., Bokkers, B., Luijten, M., Peijnenburg, A., Rijkers, D., et al., 2023. New approach methodologies: a quantitative in vitro to in vivo extrapolation case study with PFASs. Food Chem. Toxicol. 172. https://doi.org/10.1016/J.FCT.2022.113559.
Gadaleta, D., Benfenati, E., 2022. QSAR model reporting format: hepatotoxicity model (IRFMN)-v. 1.0.1. Milan. https://doi.org/10.3389/fphar.2016.00442/full.
Gautier, F., Tourneix, F., Assaf Vandecasteele, H., van Vliet, E., Bury, D., Alépée, N., 2020. Read-across can increase confidence in the Next Generation Risk Assessment for skin sensitisation: a case study with resorcinol. Regul. Toxicol. Pharmacol. 117. https://doi.org/10.1016/J.YRTPH.2020.104755.
Gilmour, N., Alépée, N., Hoffmann, S., Kern, P.S., van Vliet, E., Bury, D., et al., 2023. Applying a next generation risk assessment framework for skin sensitisation to inconsistent new approach methodology information. ALTEX - Alternat. Animal Experiment. 40, 439–451. https://doi.org/10.14573/ALTEX.2211161.
Goodrich, J.A., Walker, D.I., He, J., Lin, X., Baumert, B.O., Hu, X., et al., 2023. Metabolic signatures of youth exposure to mixtures of per- and polyfluoroalkyl substances: a multi-cohort study. Environ. Health Perspect. 131. https://doi.org/10.1289/EHP11372.
Gosling, J.P., 2013. School of Mathematics FACULTY of MATHEMATICS and PHYSICAL SCIENCES Uncertainty Quantification in Next Generation Risk Assessment.
Granados, J.C., Nigam, A.K., Bush, K.T., Jamshidi, N., Nigam, S.K., 2021. A key role for the transporter OAT1 in systemic lipid metabolism. J. Biol. Chem. 296. https://doi.org/10.1016/j.jbc.2021.100603.
Gustafson, E., Debruyne, C., De Troyer, O., Rogiers, V., Vinken, M., Vanhaecke, T., 2020. Screening of repeated dose toxicity data in safety evaluation reports of cosmetic ingredients issued by the Scientific Committee on Consumer Safety between 2009 and 2019. Arch. Toxicol. 94, 3723–3735. https://doi.org/10.1007/s00204-020-02868-2.
Gwinn, M.R., Axelrad, D.A., Bahadori, T., Bussard, D., Cascio, W.E., Deener, K., et al., 2017. Chemical risk assessment: traditional vs public health perspectives. Am. J. Publ. Health 107, 1032. https://doi.org/10.2105/AJPH.2017.303771.
Hammel, E., Webster, T.F., Gurney, R., Heiger-Bernays, W., 2022. Implications of PFAS definitions using fluorinated pharmaceuticals. iScience 25. https://doi.org/10.1016/J.ISCI.2022.104020.
Hammer, H., Schmidt, F., Marx-Stoelting, P., Pötz, O., Braeuning, A., 2021. Cross-species analysis of hepatic cytochrome P450 and transport protein expression. Arch. Toxicol. 95, 117. https://doi.org/10.1007/S00204-020-02939-4.
Hara E, Zeng W. Flutamide exacerbates steatosis and promotes early hepatocarcinogenesis in high-fat diet-fed non-obese steatotic rats: Insights from clustering analysis of mitophagy regulators AMBRA1 and LC3 2024. https://doi.org/10.21203/rs.3.rs-4371202/v1.
Health Canada, 2021. Science Approach Document Bioactivity Exposure Ratio : Application in Priority Setting and Risk Assessment, pp. 1–58.
Henneberger, L., Huchthausen, J., Wojtysiak, N., Escher, B.I., 2021. Quantitative in vitro-to- in vivo extrapolation: nominal versus freely dissolved concentration. Chem. Res. Toxicol. 34, 1175–1182. https://doi.org/10.1021/ACS.CHEMRESTOX.1C00037/ASSET/IMAGES/LARGE/TX1C00037_0005.JPEG.
Hewitt, M., Enoch, S.J., Madden, J.C., Przybylak, K.R., Cronin, M.T.D., 2013. Hepatotoxicity: a scheme for generating chemical categories for read-across, structural alerts and insights into mechanism(s) of action. Crit. Rev. Toxicol. 43, 537–558. https://doi.org/10.3109/10408444.2013.811215.
Hoffmann, S., Aiassa, E., Angrish, M., Beausoleil, C., Bois, F.Y., Ciccolallo, L., et al., 2022. Application of evidence-based methods to construct mechanism-driven chemical assessment frameworks. ALTEX 39, 499–518. https://doi.org/10.14573/ALTEX.2202141.
Hyötyläinen, T., Bodin, J., Duberg, D., Dirven, H., Nygaard, U.C., Orešič, M., 2021. Lipidomic analyses reveal modulation of lipid metabolism by the PFAS perfluoroundecanoic acid (PFUnDA) in non-obese diabetic mice. Front. Genet. 12, 721507. https://doi.org/10.3389/FGENE.2021.721507/FULL.
India-Aldana, S., Yao, M., Midya, V., Colicino, E., Chatzi, L., Chu, J., et al., 2023. PFAS exposures and the human metabolome: a systematic review of epidemiological studies. Curr. Pollut. Rep. 9, 510. https://doi.org/10.1007/S40726-023-00269-4.
Jones, H.M., Rowland-Yeo, K., 2013. Basic concepts in physiologically based pharmacokinetic modeling in drug discovery and development. CPT Pharmacometrics Syst. Pharmacol. 2, e63. https://doi.org/10.1038/PSP.2013.41.
Khan, E.A., Grønnestad, R., Krøkje, Å., Bartosov, Z., Johanson, S.M., Müller, M.H.B., et al., 2023. Alteration of hepato-lipidomic homeostasis in A/J mice fed an environmentally relevant PFAS mixture. Environ. Int. 173, 107838. https://doi.org/10.1016/J.ENVINT.2023.107838.
De Kock, J., Snykers, S., Ramboer, E., Demeester, S., Heymans, A., Branson, S., et al., 2011. Evaluation of the multipotent character of human foreskin-derived precursor cells. Toxicol. Vitro 25, 1191–1202. https://doi.org/10.1016/j.tiv.2011.03.013.
De Kock, J., Najar, M., Bolleyn, J., Al Battah, F., Rodrigues, R.M., Buyl, K., et al., 2012. Mesoderm-derived stem cells: the link between the transcriptome and their differentiation potential. Https://HomeLiebertpubCom/Scd 21, 3309–3323. https://doi.org/10.1089/SCD.2011.0723.
Kumar, A., Dixit, U., Singh, K., Gupta, S.P., Beg, M.S.J., Kumar, A., et al., 2021. Structure and properties of dyes and pigments. Dyes and Pigments - Novel Applications and Waste Treatment. https://doi.org/10.5772/INTECHOPEN.97104.
Kuster, C.J., Baumann, J., Braun, S.M., Fisher, P., Hewitt, N.J., Beck, M., et al., 2022. In silico prediction of dermal absorption from non-dietary exposure to plant protection products. Comput. Toxicol. 24, 100242. https://doi.org/10.1016/J.COMTOX.2022.100242.
Lee, G., Zheng, Y., Cho, S., Jang, C., England, C., Dempsey, J.M., et al., 2017. Post-transcriptional regulation of de novo lipogenesis by mTORC1-S6K1-SRPK2 signaling. Cell 171, 1545–1558.e18. https://doi.org/10.1016/J.CELL.2017.10.037.
Lester, C., Byrd, E.L., Shobair, M., Yan, G., 2023. Quantifying analogue suitability for SAR-based read-across toxicological assessment. Chem. Res. Toxicol. 36, 230–242. https://doi.org/10.1021/ACS.CHEMRESTOX.2C00311/SUPPL_FILE/TX2C00311_SI_002.XLS.
Lizarraga, L.E., Suter, G.W., Lambert, J.C., Patlewicz, G., Zhao, J.Q., Dean, J.L., et al., 2023. Advancing the science of a read-across framework for evaluation of data-poor chemicals incorporating systematic and new approach methods. Regul. Toxicol. Pharmacol. 137, 105293. https://doi.org/10.1016/J.YRTPH.2022.105293.
Lozano, E., Herraez, E., Briz, O., Robledo, V.S., Hernandez-Iglesias, J., Gonzalez-Hernandez, A., et al., 2013. Role of the plasma membrane transporter of organic cations OCT1 and its genetic variants in modern liver pharmacology. BioMed Res. Int. 2013, 13. https://doi.org/10.1155/2013/692071.
Lu, Y., Gao, K., Li, X., Tang, Z., Xiang, L., Zhao, H., et al., 2019. Mass spectrometry-based metabolomics reveals occupational exposure to per- and polyfluoroalkyl substances relates to oxidative stress, fatty acid β-oxidation disorder, and kidney injury in a manufactory in China. Environ. Sci. Technol. 53, 9800–9809. https://doi.org/10.1021/ACS.EST.9B01608/SUPPL_FILE/ES9B01608_SI_001.PDF.
Luckert, C., Braeuning, A., De Sousa, G., Durinck, S., Katsanou, E.S., Konstantinidou, P., et al., 2018. Adverse outcome pathway-driven analysis of liver steatosis in vitro: a case study with cyproconazole. Chem. Res. Toxicol. 31, 784–798. https://doi.org/10.1021/ACS.CHEMRESTOX.8B00112/SUPPL_FILE/TX8B00112_SI_001.PDF.
Luo, F., Pu, J., Su, Z., Xing, S., Wang, Q., Sun, L., 2023. The research progress of next generation risk assessment in cosmetic ingredients and the implications for traditional Chinese medicine risk assessment. Pharmacol. Res. - Mod. Chin. Med. 8, 100282. https://doi.org/10.1016/J.PRMCM.2023.100282.
Magurany, K.A., Chang, X., Clewell, R., Coecke, S., Haugabrooks, E., Marty, S., 2023. A pragmatic framework for the application of new approach methodologies in one health toxicological risk assessment. Toxicol. Sci. 192, 155. https://doi.org/10.1093/TOXSCI/KFAD012.
Maréchal, L., Laviolette, M., Rodrigue-Way, A., Sow, B., Brochu, M., Caron, V., et al., 2018. The CD36-pparγ pathway in metabolic disorders. Int. J. Mol. Sci. 19, 1529. https://doi.org/10.3390/IJMS19051529, 1529 2018;19.
Middleton, A.M., Reynolds, J., Cable, S., Baltazar, M.T., Li, H., Bevan, S., et al., 2022. Are non-animal systemic safety assessments protective? A Toolbox and workflow. Toxicol. Sci. 189, 124–147. https://doi.org/10.1093/TOXSCI/KFAC068.
Monetti, M., Levin, M.C., Watt, M.J., Sajan, M.P., Marmor, S., Hubbard, B.K., et al., 2007. Dissociation of hepatic steatosis and insulin resistance in mice overexpressing DGAT in the liver. Cell Metab. 6, 69–78. https://doi.org/10.1016/J.CMET.2007.05.005.

Montanari, F., Knasmüller, B., Kohlbacher, S., Hillisch, C., Baierová, C., Grandits, M., et al., 2020. Vienna LiverTox workspace—a set of machine learning models for prediction of interactions profiles of small molecules with transporters relevant for regulatory agencies. Front. Chem. 7, 503837. https://doi.org/10.3389/FCHEM.2019.00899/BIBTEX.

Moxon, T.E., Li, H., Lee, M.Y., Piechota, P., Nicol, B., Pickles, J., et al., 2020. Application of physiologically based kinetic (PBK) modelling in the next generation risk assessment of dermally applied consumer products. Toxicol. Vitro 63, 104746. https://doi.org/10.1016/J.TIV.2019.104746.

N, H., C, M., M, T.R., S, S., S, N., E M, K., et al., 2023. In vitro hepatic models to assess herb–drug interactions: approaches and challenges. Pharmaceuticals 16. https://doi.org/10.3390/PH16030409/S1.

Najjar, A., Kühnl, J., Lange, D., Géniès, C., Jacques, C., Fabian, E., et al., 2024. Next-generation risk assessment read-across case study: application of a 10-step framework to derive a safe concentration of daidzein in a body lotion. Front. Pharmacol. 15, 1421601. https://doi.org/10.3389/FPHAR.2024.1421601.

Natale, A., Boeckmans, J., Desmae, T., De Boe, V., De Kock, J., Vanhaecke, T., et al., 2018. Hepatic cells derived from human skin progenitors show a typical phospholipidotic response upon exposure to amiodarone. Toxicol. Lett. 284, 184–194. https://doi.org/10.1016/J.TOXLET.2017.11.014.

Neutral Red Uptake Assay SCOPE of the METHOD the Method Relates to the Method Is Situated in Basic Research Specify the Type of Cells/tissues/organs, 2022.

Nicol, B., Vandenbossche-Goddard, E., Thorpe, C., Newman, R., Patel, H., Yates, D., 2024. A workflow to practically apply true dose considerations to in vitro testing for next generation risk assessment. Toxicology 505. https://doi.org/10.1016/j.tox.2024.153826.

Niculite, C.M., Enciu, A.M., Hinescu, M.E., 2019. CD 36: focus on epigenetic and post-transcriptional regulation. Front. Genet. 10. https://doi.org/10.3389/FGENE.2019.00680.

Nigam, S.K., Bush, K.T., Martovetsky, G., Ahn, S.Y., Liu, H.C., Richard, E., et al., 2015. The organic anion transporter (OAT) family: a systems biology perspective. Physiol. Rev. 95, 83. https://doi.org/10.1152/PHYSREV.00025.2013.

OECD, 2020. Case Study on the Use of Integrated Approaches for Testing and Assessment for Systemic Toxicity Arising from Cosmetic Exposure to Caffeine Series on Testing and Assessment No. 321 JT03465717 OFDE. ENV/JM/MONO, 17 2019.

OECD, 2023. OCDE/OECD 497 OECD GUIDELINE for TESTING of CHEMICALS Defined Approaches for Skin Sensitisation.

Ojo, A.F., Xia, Q., Peng, C., Ng, J.C., 2021. Evaluation of the individual and combined toxicity of perfluoroalkyl substances to human liver cells using biomarkers of oxidative stress. Chemosphere 281. https://doi.org/10.1016/J.CHEMOSPHERE.2021.130808.

van Osdol, W.W., Novakovic, J., Le Merdy, M., Tsakalozou, E., Ghosh, P., Spires, J., et al., 2024. Predicting human dermal drug concentrations using PBPK modeling and simulation: clobetasol propionate case study. AAPS PharmSciTech 25, 1–14. https://doi.org/10.1208/S12249-024-02740-X/FIGURES/6.

Ouedraogo, G., Alexander-White, C., Bury, D., Clewell, H.J., Cronin, M., Cull, T., et al., 2022. Read-across and new approach methodologies applied in a 10-step framework for cosmetics safety assessment – a case study with parabens. Regul. Toxicol. Pharmacol. 132, 105161. https://doi.org/10.1016/J.YRTPH.2022.105161.

Pallocca, G., Moné, M.J., Kamp, H., Luijten, M., van de Water, B., Leist, M., 2022. Next-generation risk assessment of chemicals - rolling out a human-centric testing strategy to drive 3R implementation: the RISK-hunt3r project perspective. ALTEX 39, 419–426. https://doi.org/10.14573/altex.2204051.

Pan, Z., Li, G., Du, G., Wu, D., Li, X., Wang, Y., et al., 2022. The transcription factor RXRA regulates lipid metabolism in 1 duck myoblasts by the CD36 network. bioRxiv. https://doi.org/10.1101/2022.04.13.488167.

Paul Friedman, K., Gagne, M., Loo, L.H., Karamertzanis, P., Netzeva, T., Sobanski, T., et al., 2020. Utility of in vitro bioactivity as a lower bound estimate of in vivo adverse effect levels and in risk-based prioritization. Toxicol. Sci. 173, 202–225. https://doi.org/10.1093/toxsci/kfz201.

Pawar, G., Madden, J.C., Ebbrell, D., Firman, J.W., Cronin, M.T.D., 2019. In silico toxicology data resources to support read-across and (Q)SAR. Front. Pharmacol. 10, 449547. https://doi.org/10.3389/FPHAR.2019.00561/BIBTEX.

Peeters, L., Vervliet, P., Foubert, K., Hermans, N., Pieters, L., Covaci, A., 2020. A comparative study on the in vitro biotransformation of medicagenic acid using human liver microsomes and S9 fractions. Chem. Biol. Interact. 328, 109192. https://doi.org/10.1016/J.CBI.2020.109192.

Pizzo, F., Lombardo, A., Manganaro, A., Benfenati, E., 2016. A New Structure-Activity Relationship (SAR) Model for predicting drug-induced liver injury, based on statistical and expert-based structural alerts. Front. Pharmacol. 7. https://doi.org/10.3389/fphar.2016.00442.

Proença, S., Escher, B.I., Fischer, F.C., Fisher, C., Grégoire, S., Hewitt, N.J., et al., 2021. Effective exposure of chemicals in in vitro cell systems: a review of chemical distribution models. Toxicol. Vitro 73. https://doi.org/10.1016/j.tiv.2021.105133.

Punt, A., Louisse, J., Beekmann, K., Pinckaers, N., Fabian, E., van Ravenzwaay, B., et al., 2022. Predictive performance of next generation human physiologically based kinetic (PBK) models based on in vitro and in silico input data. ALTEX - Alternat. Animal Experiment. 39, 221–234. https://doi.org/10.14573/ALTEX.2108301.

Ratziu, V., Giral, P., Jacqueminet, S., Charlotte, F., Hartemann-Heurtier, A., Serfaty, L., et al., 2008. Rosiglitazone for nonalcoholic steatohepatitis: one-year results of the randomized placebo-controlled fatty liver improvement with rosiglitazone therapy (FLIRT) trial. Gastroenterology 135, 100–110. https://doi.org/10.1053/J.GASTRO.2008.03.078.

Rodrigues, R.M., De Kock, J., Branson, S., Vinken, M., Meganathan, K., Chaudhari, U., et al., 2014. Human skin-derived stem cells as a novel cell source for in vitro hepatotoxicity screening of pharmaceuticals. Stem Cell. Dev. 23, 44–55. https://doi.org/10.1089/SCD.2013.0157.

Rodrigues, R.M., Govaere, O., Roskams, T., Vanhaecke, T., Rogiers, V., De Kock, J., 2016. Gene expression data from acetaminophen-induced toxicity in human hepatic in vitro systems and clinical liver samples. Data Brief 7, 1052–1057. https://doi.org/10.1016/j.dib.2016.03.069.

Rogiers, V., Benfenati, E., Bernauer, U., Bodin, L., Carmichael, P., Chaudhry, Q., et al., 2020. The way forward for assessing the human health safety of cosmetics in the EU - workshop proceedings. Toxicology 436. https://doi.org/10.1016/j.tox.2020.152421.

Roth, M., Obaidat, A., Hagenbuch, B., 2012. OATPs, OATs and OCTs: the organic anion and cation transporters of the SLCO and SLC22A gene superfamilies. Br. J. Pharmacol. 165, 1260. https://doi.org/10.1111/J.1476-5381.2011.01724.X.

Rowland, A., Miners, J.O., Mackenzie, P.I., 2013. The UDP-glucuronosyltransferases: their role in drug metabolism and detoxification. Int. J. Biochem. Cell Biol. 45, 1121–1132. https://doi.org/10.1016/J.BIOCEL.2013.02.019.

Sadrabadi, F., Alarcan, J., Sprenger, H., Braeuning, A., Buhrke, T., 2024. Impact of perfluoroalkyl substances (PFAS) and PFAS mixtures on lipid metabolism in differentiated HepaRG cells as a model for human hepatocytes. Arch. Toxicol. 98, 507–524. https://doi.org/10.1007/S00204-023-03649-3/FIGURES/8.

Safety Assessment Division, Chemical Management Center, National Institute of Technology and Evaluation, 2023. Hazard evaluation support system integrated platform (HESS). https://www.nite.go.jp/en/chem/qsar/hess-e.html.

Sakuratani, Y., Zhang, H.Q., Nishikawa, S., Yamazaki, K., Yamada, T., Yamada, J., et al., 2013. Hazard Evaluation Support System (HESS) for predicting repeated dose toxicity using toxicological categories. SAR QSAR Environ. Res. 24, 351–363. https://doi.org/10.1080/1062936X.2013.773375.

Sand, S., von Rosen, D., Victorin, K., Falk Filipsson, A., 2006. Identification of a critical dose level for risk assessment: developments in benchmark dose analysis of continuous endpoints. Toxicol. Sci. 90, 241–251. https://doi.org/10.1093/TOXSCI/KFJ057.

SCCS opinion on Nitrosamines and secondary amines in cosmetic products. https://doi.org/10.2772/4079, 2012.

SCCS/1322/10. SCCS - Opinion on HC Yellow n° 13 2011. https://health.ec.europa.eu/scientific-committees/scientific-committee-consumer-safety-sccs/sccs-opinions_en (accessed December 5, 2023).

SCCS/1647/22, 2023. SCCS Notes of Guidance for the Testing of Cosmetic Ingredients and Their Safety Evaluation 12th Revision.

Schmeisser, S., Miccoli, A., von Bergen, M., Berggren, E., Braeuning, A., Busch, W., et al., 2023. New approach methodologies in human regulatory toxicology – not if, but how and when. Environ. Int. 178, 108082. https://doi.org/10.1016/J.ENVINT.2023.108082.

Schultz, T.W., Cronin, M.T.D., 2017. Lessons learned from read-across case studies for repeated-dose toxicity. Regul. Toxicol. Pharmacol. 88, 185–191. https://doi.org/10.1016/j.yrtph.2017.06.011.

Simon, T.W., Simons, S.S., Preston, R.J., Boobis, A.R., Cohen, S.M., Doerrer, N.G., et al., 2014. The use of mode of action information in risk assessment: quantitative key events/dose-response framework for modeling the dose-response for key events. Crit. Rev. Toxicol. 44, 17–43. https://doi.org/10.3109/10408444.2014.931925/SUPPL_FILE/931925_SUPPL.PDF.

Simulations-plus, 2017. PBPK modeling software from discovery through development, pp. 1–16.

Spires, J., 2020. Computational Modeling of Absorption from Complex Topical Formulations.

Suo, Y., Wright, N.J., Guterres, H., Fedor, J.G., Butay, K.J., Borgnia, M.J., et al., 2023. Molecular basis of polyspecific drug and xenobiotic recognition by OCT1 and OCT2. Nat. Struct. Mol. Biol. 30 (7), 1001–1011. https://doi.org/10.1038/s41594-023-01017-4, 2023;30.

Svingen, T., Villeneuve, D.L., Knapen, D., Panagiotou, E.M., Draskau, M.K., Damdimopoulou, P., et al., 2021. A pragmatic approach to adverse outcome pathway development and evaluation. Toxicol. Sci. 184, kfab113. https://doi.org/10.1093/TOXSCI/KFAB113.

Teixeira do Amaral, R., Ansell, J., Aptula, N., Ashikaga, T., Chaudhry, Q., Hirose, A., et al., 2014. In Silico-QSAR WG/Final Report REPORT for the INTERNATIONAL COOPERATION on COSMETICS REGULATION in Silico Approaches for Safety Assessment of Cosmetic Ingredients.

Tontonoz, P., Spiegelman, B.M., 2008. Fat and beyond: the diverse biology of PPARgamma. Annu. Rev. Biochem. 77, 289–312. https://doi.org/10.1146/ANNUREV.BIOCHEM.77.061307.091829.

Tozer, S., Alexander-White, C., Amin, R., Audebert, F., Barratt, C., O'Brien, J., et al., 2023. From worst-case to reality – case studies illustrating tiered refinement of consumer exposure to cosmetic ingredients. Regul. Toxicol. Pharmacol. 143, 105436. https://doi.org/10.1016/J.YRTPH.2023.105436.

Troutman, J.A., Rick, D.L., Stuard, S.B., Fisher, J., Bartels, M.J., 2015. Development of a physiologically-based pharmacokinetic model of 2-phenoxyethanol and its metabolite phenoxyacetic acid in rats and humans to address toxicokinetic uncertainty in risk assessment. Regul. Toxicol. Pharmacol. 73, 530–543. https://doi.org/10.1016/J.YRTPH.2015.07.012.

Tsakalozou, E., Alam, K., Ghosh, P., Spires, J., Polak, S., Fang, L., et al., 2023. Mechanistic modeling of drug products applied to the skin: a workshop summary report. CPT Pharmacometrics Syst. Pharmacol. 12, 575–584. https://doi.org/10.1002/PSP4.12893.

US EPA, 2016. Benchmark dose (BMD) methods | benchmark dose software (BMDS). https://19january2017snapshot.epa.gov/bmds/benchmark-dose-bmd-methods_.html#bmr.

Varga, T., Czimmerer, Z., Nagy, L., 2011. PPARs are a unique set of fatty acid regulated transcription factors controlling both lipid metabolism and inflammation. Biochim. Biophys. Acta (BBA) - Mol. Basis Dis. 1812, 1007–1022. https://doi.org/10.1016/J.BBADIS.2011.02.014.

Varma, M.V., Steyn, S.J., Allerton, C., El-Kattan, A.F., 2015. Predicting clearance mechanism in drug discovery: extended clearance classification system (ECCS). Pharm. Res. 32, 3785–3802. https://doi.org/10.1007/S11095-015-1749-4.

Verhoeven, A., van Ertvelde, J., Boeckmans, J., Gatzios, A., Jover, R., Lindeman, B., et al., 2024. A quantitative weight-of-evidence method for confidence assessment of adverse outcome pathway networks: a case study on chemical-induced liver steatosis. Toxicology 505, 153814. https://doi.org/10.1016/J.TOX.2024.153814.

Vienna LiverTox, 2020. Workspace. https://livertox.univie.ac.at/.

Villanueva, C.J., Monetti, M., Shih, M., Zhou, P., Watkins, S.M., Bhanot, S., et al., 2009. Specific role for acyl CoA:Diacylglycerol acyltransferase 1 (Dgat1) in hepatic steatosis due to exogenous fatty acids. Hepatology 50, 434–442. https://doi.org/10.1002/HEP.22980.

Vinken, M., 2015. Adverse outcome pathways and drug-induced liver injury testing. Chem. Res. Toxicol. 28, 1391. https://doi.org/10.1021/ACS.CHEMRESTOX.5B00208.

Wambaugh, J., 2024. Bioactivity:Exposure Ratio Example Comparing NAM-Based PODs to Estimates of Human Daily Intake. Durham, NC.

Wang, Z., Buser, A.M., Cousins, I.T., Demattio, S., Drost, W., Johansson, O., et al., 2021. A new OECD definition for per- and polyfluoroalkyl substances. Environ. Sci. Technol. 55, 15575–15578. https://doi.org/10.1021/ACS.EST.1C06896/ASSET/IMAGES/LARGE/ES1C06896_0002.JPEG.

Weininger, D., 1988. SMILES, a chemical language and information system: 1: introduction to methodology and encoding rules. J. Chem. Inf. Comput. Sci. 28, 31–36. https://doi.org/10.1021/CI00057A005/ASSET/CI00057A005.FP.PNG_V03.

Yamashita, F., Hashida, M., 2004. Structure-based approaches for predicting ADME properties. Drug Metabol. Pharmacokinet. 19, 327–338. https://doi.org/10.2133/dmpk.19.327.

Yasuhiko, Y., Ishigami, M., Machino, S., Fujii, T., Aoki, M., Irie, F., et al., 2022. Comparison of the lower limit of benchmark dose confidence interval with no-observed-adverse-effect level by applying four different software for tumorigenicity testing of pesticides in Japan. Regul. Toxicol. Pharmacol. 133. https://doi.org/10.1016/J.YRTPH.2022.105201.

Yen, C.L.E., Stone, S.J., Koliwad, S., Harris, C., Farese, R.V., 2008. Thematic review series: glycerolipids. DGAT enzymes and triacylglycerol biosynthesis. J. Lipid Res. 49, 2283–2301. https://doi.org/10.1194/JLR.R800018-JLR200.

Yun, Y.E., Tornero-Velez, R., Purucker, S.T., Chang, D.T., Edginton, A.N., 2021. Evaluation of quantitative structure property relationship algorithms for predicting plasma protein binding in humans. Comput. Toxicol. 17, 100142. https://doi.org/10.1016/J.COMTOX.2020.100142.

Zhai, J., Ji, B., Liu, S., Zhang, Y., Cai, L., Wang, J., 2022. In silico prediction of pharmacokinetic profile for human oral drug candidates which lack clinical pharmacokinetic experiment data. Eur. J. Drug Metab. Pharmacokinet. 47, 403–417. https://doi.org/10.1007/S13318-022-00758-9.

Zhang, X., Zhao, L., Ducatman, A., Deng, C., von Stackelberg, K.E., Danford, C.J., et al., 2023. Association of per- and polyfluoroalkyl substance exposure with fatty liver disease risk in US adults. JHEP Rep. 5. https://doi.org/10.1016/J.JHEPR.2023.100694.

Zhao, L., Zhang, X., Ducatman, A., Zhang, X., 2023. Associations between per- and polyfluoroalkyl substances and adolescent non-alcoholic fatty liver disease. J. Hepatol. 79, e208–e210. https://doi.org/10.1016/j.jhep.2023.06.016.